Point force singularities outside a drop covered with an incompressible surfactant: Image systems and their applications

Vaseem A. Shaik and Arezoo M. Ardekani

Phys. Rev. Fluids **2**, 113606 — Published 29 November 2017

DOI: 10.1103/PhysRevFluids.2.113606

Point force singularities outside a drop covered with an incompressible surfactant: Image systems & their applications

Vaseem A. Shaik and Arezoo M. Ardekani*

School of Mechanical Engineering, Purdue University,

West Lafayette, Indiana 47907, USA

(Dated: October 1, 2017)

Abstract

In this work, we derive the image flow fields for point force singularities placed outside a stationary drop covered with an insoluble, non-diffusing, and incompressible surfactant. We assume the interface to be Newtonian and use the Boussinesq-Scriven constitutive law for the interfacial stress tensor. We use this analytical solution to investigate two different problems. First, we derive the mobility matrix for two drops of arbitrary sizes covered with an incompressible surfactant. In the second example, we calculate the velocity of a swimming microorganism (modeled as a Stokes dipole) outside a drop covered with an incompressible surfactant.

* ardekani@purdue.edu

I. INTRODUCTION

Point force singularity solutions are commonly used to represent the disturbance flow field due to particles, drops and microorganisms in a low Reynolds number regime [1–3], where the inertial forces are negligible. For instance, the disturbance flow field due to particles of simple shape (e.g., sphere, spheroid or ellipsoid) in simple ambient flows (e.g., uniform flow, linear flow) or that due to particles of slender geometry can be represented by an internal distribution of point force singularities (and the higher order singularities) [2, 4]. More importantly, the far-field behavior of the disturbance flow field can be captured by a Stokeslet (flow field due to a point force) or a rotlet (flow field due to a point torque) or a stresslet (flow field due to a symmetric part of a force dipole), if the force, torque and the stresslet experienced by the particle are known [2]. This far-field behavior can be used to understand the interaction of particles, drops or microorganisms with interfaces [5–9].

In this work, we derive the image flow field due to the point force singularities placed outside a drop covered with an insoluble, non-diffusing and an incompressible surfactant, with allowance for the interfacial viscosity of the drop. This solution can be used to understand the pair hydrodynamic interaction of bubbles and drops in the presence of surfactants in bubbly flows and emulsion flows, respectively. It can also be used to investigate bacterial dynamics in the vicinity of oil drops; an analysis that is essential in order to understand the mechanism of bioremediation of insoluble hydrocarbons released in an oil spill. In the event of an oil spill, surfactants are often used to break down the 'heavier' oil components into tiny drops ($O\left(100-1000\right)\mu$m), which act as a carbon source for marine bacteria [10]. Therefore, it is important to understand the hydrodynamic interactions between bacteria and surfactant-laden drops, as a first step towards answering vital questions related to the process of bioremediation in oil spills. Also, the distribution of bacteria near bubbles is important in marine environments or in food cleaning procedures when cavitation bubbles are used to clean infectious bacteria from surface of food products [11].

Non-uniform distribution of surfactant (which leads to the non-uniform interfacial tension), caused by fluid flow near an insoluble surfactant laden interface, significantly alters the physics, e.g., the velocity of a force-free drop or the drag experienced by a drop. This fluid flow can be due to (i) externally applied force (e.g., gravity), (ii) externally imposed flow field, or (iii) hydrodynamic interactions with other particles. Among these, the buoy-

ancy (gravity) driven motion of drops covered with surfactants in an unbounded quiescent fluid is well understood [1, 12]. There is a recent attraction to the motion of force-free, surfactant-laden-drops in an unbounded externally imposed flow field. One interesting observation is the cross-stream migration of a non-deforming surfactant laden spherical drop (towards the centerline of the flow) in an unbounded plane/cylindrical Poisuelle flow. Hanna and Vlahovska's work [13] was the first to observe this and they focused on the limits of large Marangoni number, Ma (ratio of Marangoni forces to the viscous forces) or large viscosity ratio of the drops, neglecting any surface diffusivity of the surfactant. Schwalbe *et al.* [14] studied the influence of the interfacial viscosity of the drops, where the interface is assumed to be Newtonian and the Boussinesq-Scriven constitutive law is used for the interfacial stress tensor. Pak *et al.* [15] studied the effect of surface diffusivity of the surfactant in the limit of large diffusivity (surface Péclet number, $Pe_S \ll 1$, where Pe_S is the ratio of surface advection of the surfactant to its surface diffusion).

A lot of work has been done on the interaction of particles/drops with surfactant-laden-interfaces. Depending on the shape of the interface, one can classify these works into two categories. The first category deals with the motion of particles near a plane interface covered with a surfactant. For instance, Blawzdziewicz *et al.* [16] developed a method to find the image of an arbitrary flow field from a plane interface covered with an incompressible, insoluble and non-diffusing surfactant. They used this method to find the image of a Stokeslet, which was further utilized in deriving the mobility of a rigid sphere near a surfactant-laden interface. Recently, Lopez and Lauga [8] studied the dynamics of swimming microorganisms near a plane interface covered with an incompressible surfactant. Modeling the microorganisms with a force dipole or a rotlet dipole, they explained the attraction/repulsion of microorganisms and their swimming in circles near such complex interfaces. These two studies included the effects of interfacial viscosity. The second category deals with the interaction of two or more spherical surfactant-laden-drops. For instance, Blawzdziewicz *et al.* [17] derived the general solution of creeping flow equations surrounding a spherical drop covered with an insoluble and incompressible surfactant ($Ma \to \infty$). This solution was then used to derive the pairwise mobility functions which were further utilized to determine the collision efficiencies of two equal-sized bubbles covered with a surfactant in linear flows. In the same limit of Ma, Ramirez *et al.* [18] studied the effect of buoyancy on the interaction of neutrally buoyant rigid spheres (located outside the drop) with surfactant-covered bubbles,

in the context of microflotation. Following the procedure of Ramirez *et al.* [18], Rother and Davis [19] studied the buoyancy induced coalescence of two drops (of arbitrary size) covered with an incompressible surfactant. These three works considered the additional influence of Brownian motions and van der Walls attraction on the hydrodynamic interactions. Furthermore, Blawzdziewicz *et al.* [20] studied the rheology of a dilute suspension of spherical drops covered with surfactants, subjected to linear flows. They focused on the limit where the redistribution of surfactant on the drop is significant $Ma \sim O(1)$. They observed that the presence of surfactant can give rise to shear-thinning behavior with non-zero values of first and second normal stress differences. Extension of this work to time-dependent flows was carried out by Vlahovska *et al.* [21]. In the same limit of Ma, Cristini *et al.* [22] studied the near contact motion of surfactant covered spherical drops using lubrication theory. Also, Zinchenko *et al.* [23] studied the gravity induced collision efficiencies of two spherical drops covered with compressible surfactants (valid for arbitrary Ma and Pe_S). An intriguing result of this work is that the surfactant enhances the coalescence of drops of equal size. These works consider a linear relationship between interfacial tension and surfactant concentration and they neglect the influence of interfacial viscosity.

Mechanisms other than fluid flows can cause the non-uniform distribution of surfactants which thereby lead to the self-propulsion of particles in quiescent fluids. For instance, either during initial stages of micelle adsorption on the surface of a clean drop or by using a non-uniform mixture of two surfactants, one can observe the gradients in the surfactant concentration and consequently the interfacial tension on the surface of the drop and this propels the drop [24]. A second example is the Marangoni propulsion [25] of interface bound particles due to the release of an insoluble surface active agent. For a simple shape of these particles residing on a flat interface, such as a thin disc, Lauga and Davis derived analytical expressions for the translational velocity due to the release of surfactants [26]. Later, Masoud and Stone derived such expressions for oblate and prolate spheroidal particles using the Lorentz reciprocal theorem [27].

A traditional approach to derive the mobility of particles near a plane interface is (i) to derive the image systems of point force singularities near a *plane* interface [28–30] and then (ii) to apply the Faxén's law to a suitable combination of the images of these point force singularities. This approach is general since, once we know the images of point force singularities, we can readily derive the mobility of a rigid sphere, drop or even a swimming

microorganism near a plane interface [8, 9]. Kim and Karilla [2] used this approach to derive the mobility functions for two rigid *spheres* of arbitrary sizes while Fuentes *et al.* [31, 32] derived the mobility functions for two *spherical* drops with clean interfaces. Following this analogy, we derive the image systems for point force singularities and higher order singularities placed outside a drop covered with an incompressible surfactant, including the effects of interfacial viscosity, in Sections II and III, respectively. We thereafter, illustrate the use of the images of point force singularities by providing two examples in Sections IV and V. The first example concerns the mobility functions for two spherical drops (of arbitrary sizes) covered with an incompressible surfactant. For this purpose, we require the Faxén's laws for a spherical drop covered with an incompressible surfactant, which are derived in Appendix B. In the second example, we derive the velocity of a swimming microorganism outside a stationary drop covered with an incompressible surfactant. A brief discussion on the incompressible surfactant film is provided in Appendix A.

II. POINT FORCE OUTSIDE A DROP COVERED WITH AN INCOMPRESSIBLE SURFACTANT

In this section, we derive the image flow field due to a point force outside a stationary spherical drop covered with an insoluble, non-diffusing and incompressible surfactant. Assuming the interface to be Newtonian, we use the Boussinesq-Scriven constitutive law [33, 34] for modeling the interfacial viscous stresses. For deriving the image flow field, we use the multipole representation of the Lamb's general solution [35]. Kim and Karrila [2] used this method to derive the image of point force singularities near a rigid sphere while Fuentes *et al.* [31, 32] used it to derive the images outside a drop with a clean interface, without any interfacial viscosity. Recently, Daddi-Moussa-Ider and Gekle [36] used this method to derive the images of a point force outside a spherical elastic membrane for axisymmetric configurations.

Consider a point force $\mathbf{F}$ located at $\mathbf{x}_2$ outside a drop, whose center is at $\mathbf{x}_1$ (see Fig. 1). Scaling the distances by the radius of the drop, the flow fields inside and outside the drop are governed by Stokes equations and incompressibility conditions

$$-\nabla p^{(e)} + \mu_e \nabla^2 \mathbf{v}^{(e)} = -\mathbf{F}\delta\left(\mathbf{x}-\mathbf{x}_2\right), \ \nabla\cdot\mathbf{v}^{(e)} = 0, \ \text{ for } r_1 = \ |\mathbf{x}-\mathbf{x}_1| > 1, \tag{1}$$

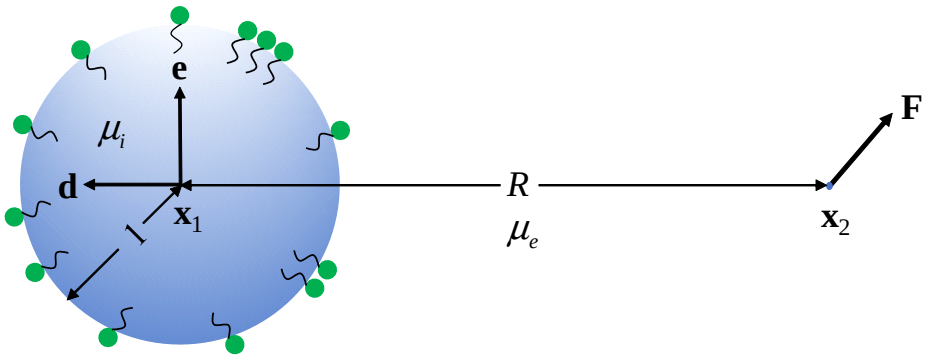

FIG. 1: Point force outside a surfactant covered drop and the associated coordinate system

$$\mu_i \nabla^2 \mathbf{v}^{(i)} = \nabla p^{(i)}, \; \nabla \cdot \mathbf{v}^{(i)} = 0, \text{ for } |\mathbf{x} - \mathbf{x}_1| < 1, \tag{2}$$

where δ is the dirac-delta function. Here $\mathbf{v}^{(k)}$ and $p^{(k)}$ denote the velocity and pressure fields, while μ_k denote the dynamic viscosity of the fluid. Also, $k = i, e$ correspond to the interior and exterior of the drop, respectively. The solution of these equations should satisfy the boundary conditions on the surface of the drop given by

$$v_r^{(e)} = v_r^{(i)} = 0, \tag{3}$$

$$\mathbf{v}_S = \boldsymbol{\Delta} \cdot \mathbf{v}^{(e)} = \boldsymbol{\Delta} \cdot \mathbf{v}^{(i)}, \tag{4}$$

$$\nabla_S \cdot \mathbf{v}_S = 0, \tag{5}$$

$$\mathbf{e}_r \cdot \left(\mathbf{T}^{(i)} - \mathbf{T}^{(e)} \right) \cdot \boldsymbol{\Delta} = \nabla_S \sigma + \mu_S \left(\frac{2\mathbf{v}_S}{r_1^2} + \mathbf{e}_\theta \frac{1}{r_1 \sin(\theta)} \frac{\partial \varpi}{\partial \phi} - \mathbf{e}_\phi \frac{1}{r_1} \frac{\partial \varpi}{\partial \theta} \right), \tag{6}$$

where $\boldsymbol{\Delta} = \mathbf{I} - \mathbf{e}_r \mathbf{e}_r$, $\mathbf{I}$ is the identity tensor, $(\mathbf{e}_r, \mathbf{e}_\theta, \mathbf{e}_\phi)$ and (v_r, v_θ, v_ϕ) are the unit vectors and the components of the velocity vector in the radial, polar and azimuthal directions with the origin at the center of the drop. $\mathbf{T}^{(i)}$ and $\mathbf{T}^{(e)}$ represent the stress tensors in the inner and outer fluids, σ denotes the interfacial tension, and μ_S denotes the interfacial shear viscosity. ∇_S is the surface gradient operator given by $\nabla_S = \boldsymbol{\Delta} \cdot \nabla$ and $\varpi = \frac{1}{r_1 \sin(\theta)} \left(\frac{\partial v_\theta}{\partial \phi} - \frac{\partial}{\partial \theta} \left(\sin(\theta) v_\phi \right) \right)$. As the drop is not deforming, Eq. (3) states that the radial velocity is zero at the drop surface. Also, Eq. (4) states that the tangential velocity $(\mathbf{v}_S)$ is continous across the interface of the drop. The surface transport equation [37] of an insoluble, non-diffusing, incompressible surfactant reduces to Eq. (5) [8, 16] (see Appendix A for details). Using the Boussenisq-Scriven constitutive law along with Eq. (5) for the surface viscous stresses $\boldsymbol{\tau}_S$, the surface divergence of surface viscous stress $\nabla_S \cdot \boldsymbol{\tau}_S$ for a spherical interface reduces to that given on the right hand side of Eq. (6).

Since Eqs. (1)-(6) are linear, we just need to solve for two orientations of the point force to derive the flow field for all possible orientations of the point force. One such orientation of the point force corresponds to an axisymmetric configuration, i.e. point force is oriented along the line joining $\mathbf{x}_1$ and $\mathbf{x}_2$ or $\mathbf{F} \parallel \mathbf{d}$, where $\mathbf{d} = (\mathbf{x}_1 - \mathbf{x}_2) / |\mathbf{x}_1 - \mathbf{x}_2|$. The other configuration corresponds to a transverse or asymmetric configuration, where $\mathbf{F} \perp \mathbf{d}$. For axisymmetric configuration, Eq. (5) implies $\mathbf{v}_S = \mathbf{0}$. Hence the image flow field due to an axisymmetric Stokeslet outside a drop covered with an incompressible surfactant is the same as that due to an axisymmetric Stokeslet outside a rigid sphere. Such a similarity between the images of an axisymmetric Stokeslet near a plane interface covered with an incompressible surfactant and that near a rigid wall was already noted by Blawzdziewicz *et al.* [16]. Kim and Karrila have derived the images due to a Stokeslet outside a rigid sphere [2]. Hence, we do not repeat this calculation but simply use their results in the next few sections of this work. In this section, we therefore focus on deriving the image due to a transverse Stokeslet. Utilizing the linearity of the problem, we write the flow field outside the drop as a sum of the Stokeslet and its image ($\mathbf{v}^*$)

$$\mathbf{v}^{(e)} = \mathbf{F}^{\perp} \cdot \left[\mathscr{G} \left(\mathbf{x} - \mathbf{x}_2 \right) / 8\pi\mu_e \right] + \mathbf{v}^*, \tag{7}$$

where $\mathscr{G}$ is the free space Green's function of the Stokes equations, the point force in the transverse problem is denoted by $\mathbf{F}^{\perp}$, $\mathbf{F}^{\perp} = F^{\perp}\mathbf{e}$ and $\mathbf{e}$ is perpendicular to $\mathbf{d}$.

We hereby derive the solution of this problem, following these four steps [31, 32]:

1. We write the Stokeslet in terms of harmonics based at $\mathbf{x}_2$, which are then transformed to the harmonics based at $\mathbf{x}_1$ using a Taylor series expansion about $\mathbf{x}_1$ (or more generally using an addition theorem). Using the properties of spherical harmonics, one can arrive at the following expression for the Stokeslet

$$\begin{aligned}
\mathbf{F}^{\perp} \cdot \mathscr{G} \left(\mathbf{x} - \mathbf{x}_2 \right) = & \sum_{n=0}^{\infty} \left[(1-n) R^{-(n+1)} r_1^{2n+1} + \frac{(2n+1)(n+1)}{(2n+3) R^{n+3}} r_1^{2n+3} \right] \mathbf{F}^{\perp} \frac{(\mathbf{d} \cdot \nabla)^n}{n!} \frac{1}{r_1} \\
& + \sum_{n=0}^{\infty} \left[\frac{R^{-(n+3)}}{(2n+3)} r_1^{2n+5} - \frac{R^{-(n+5)}}{(2n+7)} r_1^{2n+7} \right] \nabla \left(\mathbf{F}^{\perp} \cdot \nabla \right) \frac{(\mathbf{d} \cdot \nabla)^n}{n!} \frac{1}{r_1} \\
& - \sum_{n=0}^{\infty} \left[R^{-(n+2)} r_1^{2n+3} - \frac{(2n+3)}{(2n+5)} R^{-(n+4)} r_1^{2n+5} \right] (\mathbf{t} \times \nabla) \frac{(\mathbf{d} \cdot \nabla)^n}{n!} \frac{1}{r_1},
\end{aligned} \tag{8}$$

where $R = |\mathbf{x}_1 - \mathbf{x}_2|$ and $\mathbf{t} = \mathbf{F}^{\perp} \times \mathbf{d}$.

2. We then write the image flow field in terms of the multipole expansion about $\mathbf{x}_1$ as given in Eq. (9) which is eventually written in terms of harmonics based at $\mathbf{x}_1$ as given in Eq. (10)

$$\begin{aligned}\mathbf{v}^* =&\mathbf{F}^\perp \cdot \sum_{n=0}^{\infty}\left(A_n^\perp \frac{(\mathbf{d}\cdot\nabla)^n}{n!}\frac{\mathscr{G}(\mathbf{x}-\mathbf{x}_1)}{8\pi\mu_e} + B_n^\perp \frac{(\mathbf{d}\cdot\nabla)^n}{n!}\nabla^2\frac{\mathscr{G}(\mathbf{x}-\mathbf{x}_1)}{8\pi\mu_e}\right)\\ &+\sum_{n=0}^{n=\infty}\left(C_n^\perp \frac{(\mathbf{d}\cdot\nabla)^n}{n!}\frac{(\mathbf{t}\times\nabla)}{8\pi\mu_e}\frac{1}{r_1}\right) - \left(C_0^\perp - A_1^\perp\right)\frac{(\mathbf{t}\times\nabla)}{8\pi\mu_e}\frac{1}{r_1}.\end{aligned} \tag{9}$$

$$\begin{aligned}\mathbf{v}^* =&\sum_{n=0}^{\infty} A_n^\perp\left[1-n+\frac{(2n+1)(n+1)}{(2n+3)}\right]\mathbf{F}^\perp\frac{(\mathbf{d}\cdot\nabla)^n}{n!}\frac{1}{8\pi\mu_e r_1}\\ &+\sum_{n=0}^{\infty}\left[\frac{A_n^\perp r_1^2}{2n+3} - \frac{A_{n+2}^\perp}{2n+7} - 2B_n^\perp\right]\nabla\left(\mathbf{F}^\perp\cdot\nabla\right)\frac{(\mathbf{d}\cdot\nabla)^n}{n!}\frac{1}{8\pi\mu_e r_1}\\ &+\sum_{n=1}^{\infty}\left(C_n^\perp - A_{n+1}^\perp\right)(\mathbf{t}\times\nabla)\frac{(\mathbf{d}\cdot\nabla)^n}{n!}\frac{1}{8\pi\mu_e r_1}\\ &+\sum_{n=0}^{\infty}\frac{(2n+3)}{(2n+5)}A_{n+1}^\perp(\mathbf{t}\times\nabla)\frac{(\mathbf{d}\cdot\nabla)^n}{n!}\frac{1}{8\pi\mu_e r_1},\end{aligned} \tag{10}$$

where $A_n^\perp$, $B_n^\perp$, $C_n^\perp$ are the unknown constants determining the image flow field.

3. We thereafter write the flow field interior to the drop using Lamb's general solution. The connection between the Lamb's general solution and the multipole expansion is then used to write this flow field in terms of harmonics based at $\mathbf{x}_1$ as

$$\mathbf{v}^{(i)} = \sum_{n=1}^{\infty}\left\{\begin{array}{l} c_n^\perp\left(r_1^{2n-1}(\mathbf{t}\times\nabla)\frac{(\mathbf{d}\cdot\nabla)^{n-1}}{(n-1)!}\frac{1}{r_1} + (2n-1)r_1^{2n-3}(\mathbf{t}\times(\mathbf{x}-\mathbf{x}_1))\frac{(\mathbf{d}\cdot\nabla)^{n-1}}{(n-1)!}\frac{1}{r_1}\right)\\ +b_n^\perp\left(r_1^{2n+1}\nabla(\mathbf{F}\cdot\nabla)\frac{(\mathbf{d}\cdot\nabla)^{n-1}}{n!}\frac{1}{r_1} + (2n+1)r_1^{2n-1}(\mathbf{x}-\mathbf{x}_1)(\mathbf{F}\cdot\nabla)\frac{(\mathbf{d}\cdot\nabla)^{n-1}}{n!}\frac{1}{r_1}\right)\\ +a_n^\perp\left(\begin{array}{l}\frac{(n+3)}{2}r_1^{2n+3}\nabla(\mathbf{F}\cdot\nabla)\frac{(\mathbf{d}\cdot\nabla)^{n-1}}{n!}\frac{1}{r_1}\\ +\frac{(n+1)(2n+3)}{2}r_1^{2n+1}(\mathbf{x}-\mathbf{x}_1)(\mathbf{F}\cdot\nabla)\times\frac{(\mathbf{d}\cdot\nabla)^{n-1}}{n!}\frac{1}{r_1}\end{array}\right)\end{array}\right\}, \tag{11}$$

where $a_n^\perp$, $b_n^\perp$, $c_n^\perp$ are the unknown constants determining the flow field inside the drop.

4. As a final step in this method, we apply the boundary conditions to determine the unknown coefficients $A_n^\perp, B_n^\perp, C_n^\perp, a_n^\perp, b_n^\perp$ and $c_n^\perp$. Using Eq. (3) of the vanishing radial velocity on the surface of the drop, we obtain the following two equations

$$\frac{(n+1)}{2}a_n^\perp + b_n^\perp - c_{n+1}^\perp = 0, \tag{12}$$

$$\frac{(n+3)}{(2n+3)}A_{n+1}^\perp - \frac{(n+1)}{(2n-1)}A_{n-1}^\perp + 2(n+1)B_{n-1}^\perp - C_n^\perp = \frac{n}{(2n+3)}\frac{1}{R^{n+2}} - \frac{(n-2)}{(2n-1)}\frac{1}{R^n}. \tag{13}$$

After applying Eq. (4) to satisfy the continuity of tangential velocity across the interface, we obtain the following two conditions

$$\begin{aligned} -\frac{(n+3)}{2n}a_n^{\perp} - \frac{1}{n}b_n^{\perp} + \frac{1}{n}c_{n+1}^{\perp} - \frac{c_{n+3}^{\perp}}{(n+2)} - \frac{nA_{n+1}^{\perp}}{(2n+3)(n+2)} \\ +\frac{(n-2)}{(2n-1)n}A_{n-1}^{\perp} - 2B_{n-1}^{\perp} = -\frac{(n-2)}{(2n-1)n}\frac{1}{R^n} + \frac{n}{(2n+3)(n+2)}\frac{1}{R^{n+2}}, \end{aligned} \tag{14}$$

$$\frac{(n+1)}{(n+2)}c_{n+3}^{\perp} - \frac{2}{(n+2)}A_{n+1}^{\perp} + C_n^{\perp} = \frac{2}{(n+2)}\frac{1}{R^{n+2}}. \tag{15}$$

The surface divergence of the surface flow field is zero, thus Eq. (5) applied to the flow field interior to the drop gives the following condition

$$\left(\frac{n+3}{2}\right)a_n^{\perp} + b_n^{\perp} - c_{n+1}^{\perp} = 0. \tag{16}$$

Lastly, in order to satisfy the tangential stress boundary condition (Eq. (6)), one should expand the interfacial tension in terms of surface spherical harmonics and derive two equations from Eq. (6). Noting that $\mathbf{e}_r \cdot \nabla \times \nabla_S \sigma = 0$, we operate $\mathbf{e}_r \cdot \nabla \times$ on Eq. (6) and derive the following equation

$$\begin{aligned} \left(c_{n+3}^{\perp}\lambda - C_n^{\perp}\right)n^2 + \left(c_{n+3}^{\perp}\lambda - 2R^{-n-2} - 5C_n^{\perp} + 2A_{n+1}^{\perp}\right)n \\ -6C_n^{\perp} + 6A_{n+1}^{\perp} = -\beta n c_{n+3}^{\perp}(n+3)(n+1), \end{aligned} \tag{17}$$

where $\beta = \mu_S/(\mu_e a)$ and $\lambda = \mu_i/\mu_e$. Now, we can solve Eqs. (12)-(17) to directly determine the image flow field and the flow inside the drop. By using these flow fields, one can determine the interfacial tension satisfying Eq. (6). Note that we use the general approach of expanding the interfacial tension in terms of surface spherical harmonics in Appendix B to derive Faxén's laws for a drop covered with an incompressible surfactant.

Solving Eqs. (12)-(17), we derive the explicit expressions for the unknown coefficients $A_n^{\perp}$, $B_n^{\perp}$, $C_n^{\perp}$, $a_n^{\perp}$, $b_n^{\perp}$, and $c_n^{\perp}$ as follows

$$a_n^{\perp} = 0, \tag{18}$$

$$b_n^{\perp} = c_{n+1}^{\perp}, \tag{19}$$

$$c_n^{\perp} = \frac{(4n-6)}{(n-2)\left[\beta n^2 + (-3\beta + \lambda + 1)n - 3\lambda\right]}\frac{1}{R^{n-1}}, \tag{20}$$

$$A_n^{\perp} = \frac{(-2n^2-3n-1)R^{-n-3} + (2n^2+n-3)R^{-n-1}}{2n+4}, \tag{21}$$

$$B_n^{\perp} = \frac{\left[\begin{array}{l} (n+3)(n+2)(n+1)(\beta n^2+(5\beta+\lambda+1)n+4\beta+\lambda+4)R^{-n-5} \\ -2\left(\begin{array}{l}\beta n^4+(10\beta+\lambda+1)n^3+(32\beta+6\lambda+9)n^2 \\ +(29\beta+8\lambda+27)n-12\beta-3\lambda+28\end{array}\right)(n+1)R^{-n-3} \\ +(n+4)(n-1)(n+3)(\beta n^2+(5\beta+\lambda+1)n+4\beta+\lambda+4)R^{-n-1}\end{array}\right]}{4(n+4)(n+3)(n+2)(\beta n^2+(5\beta+\lambda+1)n+4\beta+\lambda+4)}, \tag{22}$$

$$C_n^{\perp} = -\frac{\left(\begin{array}{l}(\beta n^2+3+(3\beta+\lambda+1)n)(n+2)R^{-n-4} \\ -(\beta n^2+(5\beta+\lambda+1)n+6\beta+2\lambda+3)nR^{-n-2}\end{array}\right)(2n+3)}{(n+3)(\beta n^2+3+(3\beta+\lambda+1)n)(n+2)}. \tag{23}$$

From the multipole representation of the image flow field, Eq. (9), we know that the hydrodynamic force and the stresslet experienced by the drop are given by $-A_0^{\perp}\mathbf{F}^{\perp}$ and $A_1^{\perp}\left(\mathbf{F}^{\perp}\mathbf{d}+\mathbf{d}\,\mathbf{F}^{\perp}\right)/2$, respectively. But from Eq. (21) and [2], we can show that

$$A_n^{\perp}\Big|_{\substack{\text{point force outside a drop covered}\\ \text{with an incompressible surfactant}}} = A_n^{\perp}\Big|_{\substack{\text{point force outside}\\ \text{a rigidsphere}}}. \tag{24}$$

Hence, we conclude that a point force outside a drop covered with an incompressible surfactant exerts a force and stresslet on the drop which are the same as those exerted on a rigid sphere in a similar configuration. This conclusion holds for all separations between the point force and the drop. This conclusion is more general since it is valid for situations such as a translating surfactant-laden-drop in an *arbitrary* flow field as shown in Appendix B, where we also provide the physical reasons behind such behavior of a surfactant-laden-drop. Since the slowest decaying terms (and hence dominant in the far-field) in the multipole expansion of the image flow field are those due to the force and stresslet experienced by the drop, we expect that the flow field far away from the surfactant-laden-drop to be same as that outside a rigid sphere in the similar configuration. This observation is merely a consequence of the earlier observation - a surfactant-laden-drop experiencing the same force and stresslet as that of a rigid sphere due to a point force outside it. For the flow field close to a surfactant-laden-drop, the higher order terms in the multipole expansion of the image flow field (which depend on the viscosity ratio and the interfacial viscosity) become important due to which, this flow field is different from that near a rigid sphere in a similar configuration. Note that for the limiting values, λ or $\beta \to \infty$, all of these expressions for $A_n^{\perp}$, $B_n^{\perp}$, $C_n^{\perp}$, $a_n^{\perp}$, $b_n^{\perp}$ and $c_n^{\perp}$ approach the corresponding expressions for a rigid sphere as expected.

III. HIGHER ORDER SINGULARITIES OUTSIDE A DROP COVERED WITH AN INCOMPRESSIBLE SURFACTANT

In this section, we summarize the approach used for deriving the images of higher order singularities such as a Stokes dipole and a degenerate quadrupole from a drop covered with an incompressible surfactant.

A. Image of a Stokes dipole

We derive the images of a Stokes dipole by operating ∇_2 on the images of Stokeslet outside a drop covered with an incompressible surfactant, where ∇_2 denotes the gradient with respect to the location of the singularity. We hereby summarize the necessary operations required for obtaining the images of few Stokes dipoles in Eqs. (25). As these Stokes dipoles are the only singularities required for deriving either the mobility of two drops covered with a surfactant or the velocity of a swimming microorganism near a drop covered with a surfactant, we do not report the images of other Stokes dipoles. Note that, here $\mathrm{Im}\left\{\mathbf{d}\cdot\mathscr{G}\left(\mathbf{x}-\mathbf{x}_2\right)\right\}$ denotes the image of an axisymmetric Stokeslet while $\mathrm{Im}\left\{\mathbf{e}\cdot\mathscr{G}\left(\mathbf{x}-\mathbf{x}_2\right)\right\}$ denotes the image of a transverse Stokeslet.

$$\mathrm{Im}\left\{\left(\mathbf{d}\cdot\nabla\right)\mathbf{d}\cdot\mathscr{G}\left(\mathbf{x}-\mathbf{x}_2\right)\right\}=-\left(\mathbf{d}\cdot\nabla_2\right)\mathrm{Im}\left\{\mathbf{d}\cdot\mathscr{G}\left(\mathbf{x}-\mathbf{x}_2\right)\right\} \tag{25a}$$

$$\mathrm{Im}\left\{\left(\mathbf{e}\cdot\nabla\right)\mathbf{d}\cdot\mathscr{G}\left(\mathbf{x}-\mathbf{x}_2\right)\right\}=-\left(\mathbf{e}\cdot\nabla_2\right)\mathrm{Im}\left\{\mathbf{d}\cdot\mathscr{G}\left(\mathbf{x}-\mathbf{x}_2\right)\right\}-\frac{1}{R}\mathrm{Im}\left\{\mathbf{e}\cdot\mathscr{G}\left(\mathbf{x}-\mathbf{x}_2\right)\right\} \tag{25b}$$

$$\mathrm{Im}\left\{\left(\mathbf{d}\cdot\nabla\right)\mathbf{e}\cdot\mathscr{G}\left(\mathbf{x}-\mathbf{x}_2\right)\right\}=-\left(\mathbf{d}\cdot\nabla_2\right)\mathrm{Im}\left\{\mathbf{e}\cdot\mathscr{G}\left(\mathbf{x}-\mathbf{x}_2\right)\right\} \tag{25c}$$

$$\mathrm{Im}\left\{\left(\mathbf{e}\cdot\nabla\right)\mathbf{e}\cdot\mathscr{G}\left(\mathbf{x}-\mathbf{x}_2\right)\right\}=-\left(\mathbf{e}\cdot\nabla_2\right)\mathrm{Im}\left\{\mathbf{e}\cdot\mathscr{G}\left(\mathbf{x}-\mathbf{x}_2\right)\right\}+\frac{1}{R}\mathrm{Im}\left\{\mathbf{d}\cdot\mathscr{G}\left(\mathbf{x}-\mathbf{x}_2\right)\right\} \tag{25d}$$

B. Image of a degenerate quadrupole

Starting with the representation of the flow field as a sum of degenerate quadrupole and its image described in Eq. (26), we use the solution methodology analogous to Section II to derive the unknown coefficients in the image flow and the flow field interior to the drop. We denote the coefficients which appear in the image flow field of an axisymmetric and transverse degenerate quadrupole as $\left(A_n^{\parallel Q},B_n^{\parallel Q},C_n^{\parallel Q}\right)$ and $\left(A_n^{\perp Q},B_n^{\perp Q},C_n^{\perp Q}\right)$, respectively.

As these coefficients are the same as those of a rigid sphere, we note that the flow fields both inside and outside of a drop covered with an incompressible surfactant due to a degenerate quadrupole located outside the drop are same as those of flow fields due to a degenerate quadrupole outside a rigid sphere.

$$\mathbf{v} = \mathbf{F} \cdot \left[\nabla^2 \mathscr{G}\left(\mathbf{x} - \mathbf{x}_2\right)/8\pi\mu_e\right] + \mathbf{v}^* \tag{26}$$

The image flow field from a surfactant-laden-drop can be written as a combination of surface irrotational flow (which is the same as that due to a rigid sphere) and a surface solenoidal flow (see Appendix B). The image of a degenerate quadrupole from a surfactant-laden-drop is surface irrotational (i.e., the surface solenoidal part of the image flow field is zero), and the entire image flow field from the surfactant-laden-drop is the same as that from a rigid sphere.

IV. MOBILITY FUNCTIONS FOR TWO DROPS COVERED WITH AN INCOMPRESSIBLE SURFACTANT

A. A small drop near a large drop

As a first application of the image flow fields of point force singularities outside a drop covered with an incompressible surfactant, we derive the mobility matrix for hydrodynamic interactions between a large drop (radius a) and a small drop (radius b) accurate to $O\left(\delta^5\right)$, where $\delta = b/a \ll 1$. As this matrix for axisymmetric configurations is the same as that for two rigid spheres [2], we only focus on the transverse configuration (the velocity of the drops is perpendicular to the line joining their centers). For this purpose, we use a procedure similar to the method of reflections, where we consider the entire multipole expansion when the images are taken with respect to the large drop. However, we truncate this multipole expansion to a prescribed order in b/R when taking images with respect to a small drop. We require Faxén's laws for a drop covered with a surfactant along with singularity representation of the flow field due to a translating drop covered with a surfactant to be able to use the method of reflections. From the derivation of Faxén's laws presented in Appendix B, we conclude that the Faxén's laws for the force and stresslet experienced by a drop covered with an incompressible surfactant are the same as those of a rigid sphere. On the other hand, the Faxén's laws for the torque experienced by a drop covered with a surfactant is the same

as that of a drop with a clean interface and without any interfacial viscosity, namely the drop experiences zero hydrodynamic torque. Also, since the flow field due to a translating drop covered with a surfactant is axisymmetric, it behaves as a rigid sphere (namely fluid inside the drop with respect to itself is stationary) and hence the singularity representation of the flow field due to a translating drop covered with a surfactant is the same as that of a translating rigid sphere. The mobility functions, which relate the velocities of the drops with the forces acting on them, are written as [2]

$$\begin{pmatrix} \mathbf{U}_1 \\ \mathbf{U}_2 \end{pmatrix} = \frac{1}{\mu_e} \begin{pmatrix} y^a_{11} & y^a_{12} \\ y^a_{21} & y^a_{22} \end{pmatrix} \begin{pmatrix} \mathbf{F}^e_1 \\ \mathbf{F}^e_2 \end{pmatrix}. \tag{27}$$

1. Mobility functions y^a_{12} and y^a_{22}

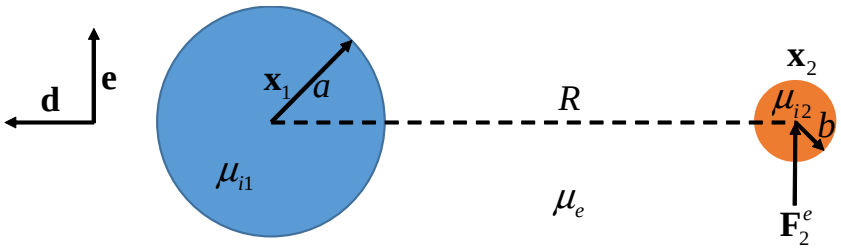

FIG. 2: Schematic used for deriving the mobility functions (y^a_{12}, y^a_{22}) for the transverse motion of the drops. Here, an external force, $\mathbf{F}^e_2$ is acting on the small drop while no external force is applied on the large drop.

For deriving the mobility functions y^a_{12} and y^a_{22}, we apply a force $\mathbf{F}^e_2$ on drop 2 and zero force on drop 1 (see Fig. 2). At zeroth reflection, the velocity of drop 2 and the flow field due to its translation are given by

$$6\pi\mu_e b\mathbf{U}^{(0)}_2 = \mathbf{F}^e_2, \tag{28}$$

$$\mathbf{v}_2 = \mathbf{F}^e_2 \cdot \left(1 + \frac{b^2\nabla^2}{6}\right) \frac{\mathscr{G}\left(\mathbf{x} - \mathbf{x}_2\right)}{8\pi\mu_e}. \tag{29}$$

At the first reflection, the velocity of the drop 1 is obtained by applying the Faxén's law for force (same as that of a rigid sphere) given by Eq. (30) which reduces to Eq. (31)

$$\mathbf{U}^{(1)}_1 = \left(1 + \frac{a^2\nabla^2}{6}\right) \mathbf{v}_2|_{\mathbf{x}=\mathbf{x}_1}, \tag{30}$$

$$6\pi\mu_e b\mathbf{U}_1^{(1)} = \mathbf{F}_2^e\left[\frac{3}{4}\left(\frac{b}{R}\right)+\frac{1}{4}\left(\frac{b}{R}\right)\left(\frac{a}{R}\right)^2+\frac{1}{4}\left(\frac{b}{R}\right)^2\right]. \tag{31}$$

Up to this reflection, the velocities of drops covered with surfactants are the same as those of rigid spheres. For finding the flow field reflected from drop 1, $\mathbf{v}_{21}$, we need the images of a Stokeslet of strength $\mathbf{F}_2^e$ and a degenerate quadrupole of strength $\frac{b^2}{6}\mathbf{F}_2^e$ located at $\mathbf{x}_2$ (center of drop 2) from a force-free drop located at $\mathbf{x}_1$. The images from a force-free drop can be obtained by first deriving the force exerted by the flow fields of a Stokeslet and degenerate quadrupole on a stationary drop ($-\mathbf{F}_2^e A_0$) and then adding the flow field due to a translating drop, acted upon by an external force ($-\mathbf{F}_2^e A_0$), to the images of the aforementioned point force singularities with respect to a stationary drop (derived in Sections II and III). Hence the flow field reflected from a force-free drop 1 is given by

$$\begin{aligned}\mathbf{v}_{21} = {}& \mathbf{F}_2^e\cdot\sum_{n=0}^{\infty}\left(A_n\tfrac{(\mathbf{d}\cdot\nabla)^n}{n!}\tfrac{\mathscr{G}(\mathbf{x}-\mathbf{x})}{8\pi\mu_e}+B_n\tfrac{(\mathbf{d}\cdot\nabla)^n}{n!}\nabla^2\tfrac{\mathscr{G}(\mathbf{x}-\mathbf{x})}{8\pi\mu_e}\right)\\ &+\sum_{n=0}^{\infty}C_n\left(\mathbf{t}\times\nabla\right)\tfrac{(\mathbf{d}\cdot\nabla)^n}{n!}\tfrac{1}{8\pi\mu_e r_1}-\left(C_0-A_1\right)\left(\mathbf{t}\times\nabla\right)\tfrac{1}{8\pi\mu_e r_1}\\ &\underbrace{-\mathbf{F}_2^e A_0\cdot\left(1+\frac{a^2\nabla^2}{6}\right)\frac{\mathscr{G}\left(\mathbf{x}-\mathbf{x}\right)}{8\pi\mu_e}}_{\text{Flow added to satisfy the force-free condition for the drop}},\end{aligned} \tag{32}$$

where $A_n = A_n^{\perp}+\frac{b^2}{6}A_n^{\perp Q}$, $B_n = B_n^{\perp}+\frac{b^2}{6}B_n^{\perp Q}$ and $C_n = C_n^{\perp}+\frac{b^2}{6}C_n^{\perp Q}$. At the second reflection, drop 2 is force free. Hence its velocity is obtained by applying the Faxén's law for the force

$$\mathbf{U}_2^{(2)} = \left(1+\frac{b^2}{6}\nabla^2\right)\mathbf{v}_{21}|_{\mathbf{x}=\mathbf{x}_2}. \tag{33}$$

Using the properties of spherical harmonics, we obtain

$$6\pi\mu_e b\mathbf{U}_2^{(2)} = \mathbf{F}_2^e\begin{bmatrix}\left(\frac{b}{R}\right)\left(\frac{x^5}{16}-\frac{9}{8}\sum_{n=1}^{\infty}\frac{1+\beta_1 n^2+\left(3\beta_1+\lambda_1-\frac{1}{3}\right)n}{3+\beta_1 n^2+(3\beta_1+\lambda_1+1)n}x^{2n+3}\right)\\ +\frac{1}{8}\left(\frac{b}{R}\right)^3\sum_{n=1}^{\infty}\left(4n^2+6n-1\right)x^{2n+3}\\ -\frac{1}{48}\left(\frac{b}{R}\right)^5\sum_{n=1}^{\infty}\left(2n+1\right)\left(2n+3\right)\left(n+1\right)^2x^{2n+1}\end{bmatrix}, \tag{34}$$

where $x = a/R$. At this reflection, one can also derive the stresslet experienced by the drop covered with a surfactant using the Faxén's laws for a stresslet (same as that of a rigid sphere)

$$\mathbf{S}_2^{(2)} = \frac{20}{3}\pi\mu_e b^3\mathbf{E}_{21}|_{\mathbf{x}=\mathbf{x}_2}+O\left[(b/a)^5\right] = \mathscr{S}_2^{(2)}\left(\mathbf{F}_2^e\mathbf{d}+\mathbf{d}\mathbf{F}_2^e\right). \tag{35}$$

Here, we only include the Stokeslet component of $\mathbf{v}_{21}$ in evaluating the rate of strain field $\mathbf{E}_{21}$. The flow field reflected from drop 2 is given by the flow field due to a stresslet

$$\mathbf{v}_{212} = \left(\mathbf{S}_2^{(2)} \cdot \nabla\right) \cdot \frac{\mathscr{G}\left(\mathbf{x} - \mathbf{x}_2\right)}{8\pi\mu_e}, \tag{36}$$

where this solution is accurate to $(b/R)^4$. At the third reflection, drop 1 is also force free. Hence, we determine its velocity by applying the Faxén's law for the force given by Eq. (37) which simplifies to Eq. (38)

$$\mathbf{U}_1^{(3)} = \left(1 + \frac{a^2}{6}\nabla^2\right) \mathbf{v}_{212}|_{\mathbf{x}=\mathbf{x}_1}, \tag{37}$$

$$6\pi\mu_e b\mathbf{U}_1^{(3)} = \frac{15}{16}\left(\frac{b}{R}\right)^4 \mathbf{F}_2^e \left(-\frac{x^7}{3} + \sum_{n=1}^{\infty}(2n+3)\,\frac{1+\beta_1 n^2 + \left(3\beta_1+\lambda_1+\frac{1}{3}\right)n}{3+\beta_1 n^2+(3\beta_1+\lambda_1+1)\,n}x^{2n+5}\right). \tag{38}$$

Using the images of a Stokes dipole from a drop covered with a surfactant which was described in Section III, we find the flow field reflected from drop 1, $\mathbf{v}_{2121}$. Applying the Faxén's law for the force to drop 2, $\mathbf{U}_2^{(4)} = \mathbf{v}_{2121}|_{\mathbf{x}=\mathbf{x}_2}$, we find

$$6\pi\mu_e b\mathbf{U}_2^{(4)} = -\frac{45}{64}\left(\frac{b}{R}\right)^4 \mathbf{F}_2^e \left(\frac{x^5}{3} - \sum_{n=1}^{\infty}(2n+3)\,\frac{1+\beta_1 n^2 + \left(3\beta_1+\lambda_1+\frac{1}{3}\right)n}{3+\beta_1 n^2+(3\beta_1+\lambda_1+1)\,n}x^{2n+3}\right)^2. \tag{39}$$

Equations for the droplet velocities at various reflections, Eqs. (28), (31), (34), (38), and (39) can be used to find the mobility functions accurate to $O\left[(b/a)^5\right]$ as given below

$$\begin{aligned} 6\pi b y_{12}^a =& \delta\left(\frac{3}{4}x + \frac{1}{4}x^3\right) + \delta^3\left(\frac{1}{4}x^3\right) \\ &+ \delta^4\left[\frac{15}{16}\left(-\frac{x^{11}}{3} + \sum_{n=1}^{\infty}(2n+3)\,\frac{1+\beta_1 n^2 + \left(3\beta_1+\lambda_1+\frac{1}{3}\right)n}{3+\beta_1 n^2+(3\beta_1+\lambda_1+1)\,n}x^{2n+9}\right)\right] + O\left(\delta^6\right), \end{aligned} \tag{40}$$

$$\begin{aligned} 6\pi b y_{22}^a =& 1 + \delta\left(\frac{x^6}{16} - \frac{9}{8}\sum_{n=1}^{\infty}\frac{1+\beta_1 n^2 + \left(3\beta_1+\lambda_1-\frac{1}{3}\right)n}{3+\beta_1 n^2+(3\beta_1+\lambda_1+1)\,n}x^{2n+4}\right) + \delta^3\left(\frac{1}{8}\frac{x^8\left(x^4-9\right)}{(x-1)^3(x+1)^3}\right) \\ &- \delta^4\left[\frac{45}{64}\left(\frac{x^7}{3} - \sum_{n=1}^{\infty}(2n+3)\,\frac{1+\beta_1 n^2 + \left(3\beta_1+\lambda_1+\frac{1}{3}\right)n}{3+\beta_1 n^2+(3\beta_1+\lambda_1+1)\,n}x^{2n+5}\right)^2\right] \\ &+ \delta^5\left[\frac{1}{16}\frac{x^8\left(x^8-5x^6+11x^4+5x^2+20\right)}{(x-1)^5(x+1)^5}\right] + O\left(\delta^6\right). \end{aligned} \tag{41}$$

2. Mobility functions y^a_{21} and y^a_{11}

For deriving the mobility functions y^a_{21} and y^a_{11}, we apply an external force $\mathbf{F}^e_1$ on drop 1 and carry out the procedure outlined in the previous subsection. Doing so, we notice that $y^a_{21} = y^a_{12}$ which means the mobility matrix is symmetric for drops covered with an incompressible surfactant. Also, to an order of approximation of $O(\delta^5)$, only $\mathbf{U}^{(0)}_1$ and $\mathbf{U}^{(2)}_1$ contribute to y^a_{11}. Here, $\mathbf{U}^{(2)}_1$ can be easily derived by swapping $(1,2)$ and (a,b) in the equation for $\mathbf{U}^{(2)}_2$, Eq. (34) and truncating the resulting expression to $(b/R)^5$. Hence, the mobility function y^a_{11} is given by

$$6\pi a y^a_{11} = 1 - \delta^3\left(\frac{5}{4}x^8\right) + \delta^5\left[\frac{3}{8}\left(\frac{1}{6} - \frac{2+12\beta_2+3\lambda_2}{4+4\beta_2+\lambda_2}\right)x^6 + \frac{9}{8}x^8 - \frac{105}{16}x^{10}\right] + O\left(\delta^6\right). \quad (42)$$

All of these mobility functions approach the corresponding mobility functions for rigid spheres when either $(\beta_1,\beta_2)\to\infty$ or $(\lambda_1,\lambda_2)\to\infty$.

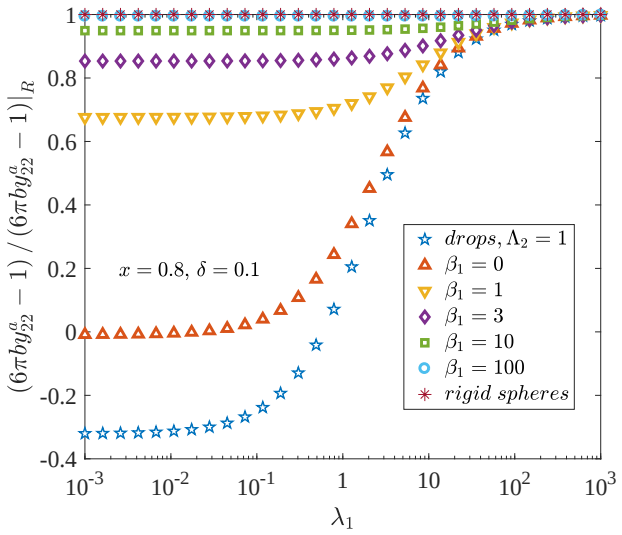

FIG. 3: Variation of $(6\pi b y^a_{22} - 1) / (6\pi b y^a_{22} - 1)|_R$ with the viscosity ratio (λ_1) and the interfacial viscosity (β_1) of the large drop. Here $\star$ $(*)$ denotes the situation of a small rigid sphere outside a large clean drop without any interfacial viscosity (rigid sphere). The other symbols denote the situation of two surfactant-laden-drops of disparate sizes. Also,

$$x = a/R = 0.8,\ \delta = b/a = 0.1 \text{ and } \Lambda_2 = \lambda_2/(1+\lambda_2)$$

From Eqs. (40), (41, and (42), we see that the mobility functions, $y^a_{12}\,(= y^a_{21})$ and y^a_{11} of two surfactant-laden-drops are identical to the corresponding mobility functions of two rigid spheres, upto an approximation of δ^3. However, the mobility function, y^a_{22} of two

surfactant-laden-drops is different from that of two rigid spheres. Also, we note that y_{22}^a does not depend on the viscosity ratio (λ_2) and the interfacial viscosity (β_2) of the small drop. So, as long as the interface of the small drop is incompressible, y_{22}^a does not depend on the identity of the small drop. To study the dependence of y_{22}^a on the viscosity ratio (λ_1) and the interfacial viscosity (β_1) of the large drop, we plot in Fig.3, the correction in y_{22}^a due to the presence of a large surfactant-laden-drop ($6\pi b y_{22}^a - 1$), normalized with the correction due to the presence of a large rigid sphere $(6\pi b y_{22}^a - 1)|_R$ for various values of λ_1 and β_1. As y_{22}^a denotes the velocity of a small drop, we see from Fig.3 that the velocity of a small drop near a large drop (with or without surfactants) is always less than that near a rigid sphere. Also, the velocity of small drop near a large clean drop is minimum and its velocity near a large surfactant-laden-drop increases with the interfacial viscosity. A similar trend is observed for the variation of the mobility of a particle near a plane interface covered with an incompressible surfactant[16].

B. Drops of similar sizes

In this section, we comment on the mobility functions of two drops covered with an incompressible surfactant, if the drops sizes are of the same order of magnitude. Noting that (i) the flow field due to an isolated translating drop covered with an incompressible surfactant (axisymmetric problem) is the same as that of an isolated translating rigid sphere and (ii) the Faxén laws for a drop covered with an incompressible surfactant are the same as those of a torque-free rigid sphere, we conclude that the far-field mobility functions of two similar sized drops covered with an incompressible surfactant are the same as those of two similar sized torque-free rigid spheres. Since the mobility functions for two torque-free rigid spheres were already derived in [2] (see chapter 8), we do not pursue this calculation further. As the flow field close to a translating surfactant-laden-drop, in an arbitrary ambient flow, is different from that near a translating torque-free rigid sphere, we expect the near-field mobility functions of two similar sized surfactant-laden-drops to be completely different from those of two similar sized torque-free rigid spheres.

Blawzdziewicz *et al.* [17] derived the mobility functions of two equal sized bubbles covered with an incompressible, insoluble and diffusing surfactant without accounting for the interfacial viscosity. For zero surfactant diffusivity, they report that their far-field mobil-

ity functions are the same as those of two torque-free rigid spheres. Our analysis, on the far-field mobility functions, not only agrees with that of Blawzdziewicz *et al.* [17] for zero viscosity ratio, interfacial viscosity and surfactant diffusivity but also generalizes the result − the far-field mobility functions of two *similar* sized surfactant-laden-drops is the same as those of two similar sized torque-free rigid spheres − to arbitrary values of viscosity ratio and interfacial viscosity.

V. SWIMMING MICROORGANISM OUTSIDE A STATIONARY DROP COVERED WITH AN INCOMPRESSIBLE SURFACTANT

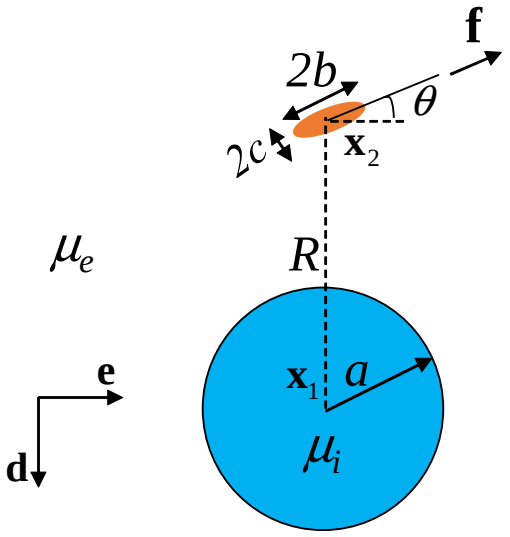

FIG. 4: Schematic: Spheroidal swimmer of aspect ratio $\gamma = b/c$ outside a stationary spherical drop of radius a. The drop has a viscosity of μ_i while the viscosity of the surrounding fluid is μ_e. The swimmer is oriented along $\mathbf{f}$. The distance between the center of the drop and the swimmer is denoted by R. The position vectors of the center of the drop and the swimmer are denoted by $\mathbf{x}_1$ and $\mathbf{x}_2$, respectively. The origin of the coordinate system is located at the center of the drop.

As a second application of image flow fields, we derive the velocity of a spheroidal microorganism swimming outside the drop covered with an incompressible surfactant (see Fig. 4). We also provide the expression for the velocity of the same microorganism swimming outside a drop with a clean interface, without any interfacial viscosity using the image flow fields

provided in [31, 32]. Flow field far away from the microorganism in an unbounded medium is represented by a parallel Stokes dipole (force and force gradient are parallel/anti-parallel to each other). Therefore, when $R-a \gg b$, the leading order velocity of the swimmer near the drop is obtained by applying Faxén's laws to the image of a Stokes dipole. So, the flow field outside a drop is written as sum of a Stokes dipole and its image

$$\mathbf{v} = -P\left(\mathbf{f}\cdot\nabla\right)\mathbf{f}\cdot\frac{\mathscr{G}\left(\mathbf{x}-\mathbf{x}_2\right)}{8\pi\mu_e} + \mathbf{v}^*, \tag{43}$$

where P is the dipole strength of the swimmer [7], $\mathbf{f}$ is the orientation of the swimmer and $\mathbf{v}^*$ is the image flow field. Here $P>0$ means the swimmer is a pusher while $P<0$ means the swimmer is a puller. We use the images of a Stokes dipole given in Section III to derive the image flow field $\mathbf{v}^*$. The translational velocity of the swimmer given by $\mathbf{U} = \mathbf{v}^*\big|_{\mathbf{x}=\mathbf{x}_2} + O\left[(b/R)^2\right]$ can be simplified to

$$\mathbf{U} = \sin^2(\theta)\,\mathbf{U}_1 - \sin(\theta)\cos(\theta)\,\mathbf{U}_2 + \cos^2(\theta)\,\mathbf{U}_3, \tag{44}$$

where $\mathbf{U}_1$, $\mathbf{U}_2$ and $\mathbf{U}_3$ for a drop covered with an incompressible surfactant are given by

$$\mathbf{U}_1 = -\frac{P}{8\pi\mu_e R^2}\frac{3x}{(-1+x)^2(x+1)^2}\mathbf{d}, \tag{45a}$$

$$\mathbf{U}_2 = -\frac{P}{8\pi\mu_e R^2}\sum_{n=0}^{\infty}\frac{3\left(2n+3\right)\left[1+\beta n^2+\left(3\beta+\lambda+\frac{1}{3}\right)n\right]x^{2n+3}}{6+2\beta n^2+\left(6\beta+2\lambda+2\right)n}\mathbf{e}, \tag{45b}$$

$$\mathbf{U}_3 = \frac{3P}{16\pi\mu_e R^2}\frac{x}{(-1+x)^2(x+1)^2}\mathbf{d}. \tag{45c}$$

The expressions for $\mathbf{U}_1$, $\mathbf{U}_2$ and $\mathbf{U}_3$ for a drop with a clean interface, without any interfacial viscosity are given by

$$\mathbf{U}_1 = -\frac{P}{8\pi\mu_e R^2}\frac{(\Lambda+2)\,x}{(-1+x)^2(x+1)^2}\mathbf{d}, \tag{46a}$$

$$\mathbf{U}_2 = -\frac{P}{8\pi\mu_e R^2}\sum_{n=0}^{\infty}\frac{3\Lambda\left(n-\Lambda+1\right)\left(2n+3\right)}{2n+6-6\Lambda}x^{2n+3}\mathbf{e}, \tag{46b}$$

$$\mathbf{U}_3 = \frac{P}{16\pi\mu_e R^2}\frac{(\Lambda+2)\,x}{(-1+x)^2(1+x)^2}\mathbf{d}, \tag{46c}$$

where $\Lambda = \lambda/(1+\lambda)$. Also, the angular velocity of the swimmer is given by

$$\boldsymbol{\omega} = \frac{1}{2}\nabla\times\mathbf{v}^*\Big|_{\mathbf{x}=\mathbf{x}_2} + \Gamma\,\mathbf{f}\times\mathbf{E}^*\big|_{\mathbf{x}=\mathbf{x}_2}\cdot\mathbf{f} + O\left[(b/R)^3\right], \tag{47}$$

where $\Gamma = (1-\gamma^2)/(1+\gamma^2)$, γ is the aspect ratio of the swimmer which is 1 for a spherical swimmer and tends to infinity for a rod shaped swimmer and $\mathbf{E}^* = \frac{1}{2}\left[\nabla \mathbf{v}^* + (\nabla \mathbf{v}^*)^T\right]$ is the rate of strain tensor of the image flow field. This expression for the angular velocity, $\boldsymbol{\omega} = \omega(\mathbf{e} \times \mathbf{d})$ can be simplified to

$$\omega = \omega^{(1)} + \Gamma \omega^{(2)}, \tag{48}$$

where $\omega^{(1)}$, $\omega^{(2)}$ for a drop covered with an incompressible surfactant are given by

$$\omega^{(1)} = \frac{3P\sin(2\theta)}{32\pi\mu_e R^3} \sum_{n=0}^{\infty} \frac{n(n+2)\left[\beta n^2 + \left(\beta+\lambda+\frac{5}{3}\right)n - 2\beta - \lambda + \frac{7}{3}\right]}{\beta n^2 + (\beta+\lambda+1)n - 2\beta - \lambda + 2} x^{2n+1}, \tag{49a}$$

$$\omega^{(2)} = -\frac{P\sin(2\theta)}{16\pi\mu_e R^3}\left(\tilde{\omega}\cos^2(\theta) + \hat{\omega}\right), \tag{49b}$$

where

$$\begin{aligned}
\tilde{\omega} =& \frac{9}{8}\frac{(6\beta+3\lambda-2)}{(2\beta+\lambda-2)}x \\
&+ \frac{3}{4}\sum_{n=0}^{\infty} \frac{n^3\beta + \left(\frac{5}{2}\beta+\lambda+3\right)n^2 + \left(-\frac{1}{2}\beta+\frac{1}{2}\lambda+\frac{17}{2}\right)n - 3\beta - \frac{3}{2}\lambda + 5}{\beta n^2 + (\beta+\lambda+1)n - 2\beta - \lambda + 2}(n+3)x^{2n+1}, \\
\hat{\omega} =& -\frac{1}{2}\frac{(6\beta+3\lambda-2)}{(2\beta+\lambda-2)}x \\
&- \frac{3}{2}\sum_{n=0}^{\infty} \frac{n^3\beta + \left(2\beta+\lambda+\frac{5}{3}\right)n^2 + \left(-\beta+\frac{14}{3}\right)n - 2\beta - \lambda + \frac{8}{3}}{\beta n^2 + (\beta+\lambda+1)n - 2\beta - \lambda + 2}(n+2)x^{2n+1}.
\end{aligned}$$

The expressions for $\omega^{(1)}$ and $\omega^{(2)}$ for a drop with a clean interface, without any interfacial viscosity are given by

$$\omega^{(1)} = \frac{3}{4}\frac{P\sin(2\theta)}{8\pi\mu_e R^3} \sum_{n=0}^{\infty} \frac{n(n+2)(-2\Lambda^2+n+1)}{n+2-3\Lambda} x^{2n+1}, \tag{50a}$$

$$\omega^{(2)} = -\frac{P\sin(2\theta)}{16\pi\mu_e R^3}\left(\tilde{\omega}\cos^2(\theta) + \hat{\omega}\right), \tag{50b}$$

where

$$\begin{aligned}
\tilde{\omega} =& \frac{27}{8}\frac{\Lambda^2 x}{(-2+3\Lambda)} \\
&- \frac{3}{4}\sum_{n=0}^{\infty} \frac{(\Lambda-2)n^2 + \left(3\Lambda^2+\frac{5}{2}\Lambda-6\right)n + \frac{3}{2}\Lambda^2 + 4\Lambda - 4}{(n+2-3\Lambda)}(n+3)x^{2n+1}, \\
\hat{\omega} =& -\frac{3}{2}\frac{\Lambda^2 x}{(-2+3\Lambda)} - \frac{3}{2}\sum_{n=0}^{\infty} \frac{n^2 + (-2\Lambda^2-\Lambda+3)n - \Lambda^2 - 2\Lambda + 2}{(n+2-3\Lambda)}(n+2)x^{2n+1}.
\end{aligned}$$

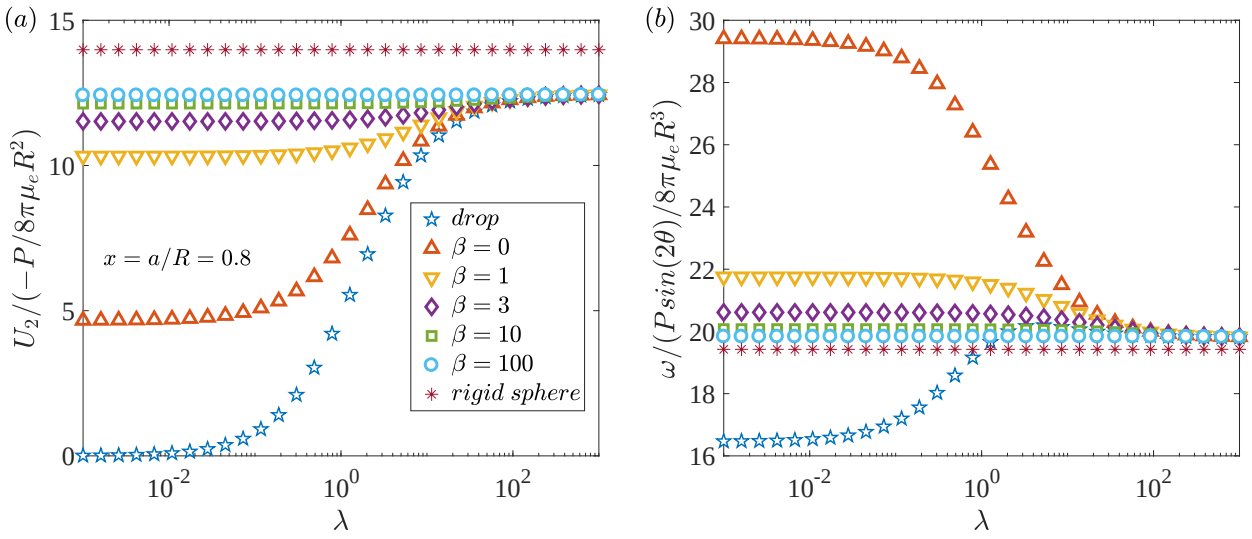

FIG. 5: Variation of (a) the dimensionless velocity of the swimmer that is normal to the line of centers and (b) dimensionless angular velocity of the spherical swimmer with the viscosity ratio (λ) and dimensionless interfacial viscosity (β). Here $\star$ ($*$) denotes the situation of the swimmer lying outside a clean drop without any interfacial viscosity (rigid sphere). The other symbols denote the situation of swimmer moving outside the surfactant-laden-drop.

In the limit $\lambda \to \infty$ ($\Lambda \to 1$) or $\beta \to \infty$, these expressions for the swimmer velocity outside a drop reduce to those outside a rigid sphere [38]. From Eqs. (44), (45a), and (45c), we see that the component of the swimmer's velocity along the line of centers ($\mathbf{U} \cdot \mathbf{d}$), outside a surfactant-laden-drop, is the same as the corresponding velocity outside a rigid sphere. The viscosity ratio of the drop and its interfacial viscosity only affect the component of the velocity that is normal to the line of centers (U_2). To understand this, we plot in Fig.5a, the dimensionless counter part of U_2 for various values of λ and β. This figure shows that, in the limit λ or $\beta \to \infty$, the velocity of the swimmer outside a drop approach its velocity outside a rigid sphere. From Eq. (46b) and also from Fig.5a, we see that a swimmer outside a bubble ($\lambda = 0$ or $\Lambda = 0$) cannot move normal ot the line of centers. So, irrespective of its orientation and the angular velocity, a puller (pusher) outside a bubble always moves towards (away from) the bubble along the line of centers. We can also see from Fig.5a that the presence of an interface reduces the velocity normal to the line of centers when compared to this velocity outside a rigid sphere. The velocity of the swimmer (normal to the line of centers)

outside a clean drop is minimum while that outside a surfactant-laden-drop increases with the interfacial viscosity. Similar to Fig.5a, we plot in Fig.5b, the variation of the angular velocity of the swimmer with the viscosity ratio and the interfacial viscosity. From Fig.5b, we see that the angular velocity of the swimmer outside a surfactant-laden-drop decreases with the interfacial viscosity and it is always larger than that outside a rigid sphere. Also, the angular velocity of the swimmer outside a clean drop can be larger or smaller than that outside a rigid sphere, depending on the viscosity ratio of the drop.

VI. CONCLUSIONS

Using the multipole representation of the Lamb's general solution, we derived the image systems for point force singularities located outside a stationary drop covered with an insoluble, non-diffusing and incompressible surfactant. Our derivation includes the role of the interfacial viscosity of the drop by assuming the interface to be Newtonian and using the Boussenisq-Scriven constitutive law for the interfacial stress tensor. We demonstrate the significance of these image systems by providing two examples. In the first example, we derive the mobility functions of two surfactant-laden drops of disparate sizes, using the method of reflections. We unveil the role of the viscosity ratio and the interfacial viscosity of the large surfactant-laden-drop on the mobility of the small surfactant-laden-drop. In the second example, we derive the velocity of the swimming microorganism (modeled as a Stokes dipole) outside (i) a surfactant-laden-drop and (ii) a clean drop without any interfacial viscosity.

Here, we summarize the range of separations between the drops or drop and singularity where the solutions presented in the manuscript are accurate. The image system of a point force or higher order singularity outside a drop is accurate for all separations between the drop and the singularity except for the singularity touching the drop. The mobility functions of two drops of disparate sizes, derived in Section IV A, is accurate for all the separations between the drops whereas the mobility functions of two drops of similar sizes, discussed in Section IV B, is accurate only for the large separations between the drops. Hence, one can use twin multipole expansions along with the addition theorem to derive the mobility functions of two similar sized drops for arbitrary separations between them. Since the flow field far away from a microorganism (swimmer) can be represented by the flow due to a force dipole placed at the center of the swimmer, the velocity of such a swimmer outside a

drop, derived in Section V where the swimmer is replaced by a force dipole, is accurate for large separations between the swimmer and the drop.

We emphasize that our derivations can be used to study the trapping characteristics [38] of bacteria near oil drops and air bubbles, in applications like bioremediation and food cleansing, respectively. One can proceed to determine the following quantities (a) critical trapping radius of the drop/bubble: minimum drop radius beyond which a bacteria near a drop/bubble gets trapped, (b) basin of attraction: space around the drop/bubble, with radius larger than the critical trapping radius, within which if a bacteria is present, gets trapped and (c) probability density function of mean trapping time: time during which a bacterium orbits around the surface of the drop/bubble before escaping. This analysis can then be used to understand the hydrodynamics induced trapping of bacteria near drops/bubbles and also the (possible) usefulness of surfactant in this trapping process.

Appendix A: Incompressible surfactant film

In this section, we derive the incompressible surfactant film condition, Eq. (5), which holds in one of the two limits − (a) large values of the Marangoni number (Ma, the ratio of tangential stresses generated at the surface by surface tension gradients to tangential stresses applied to the surface by bulk viscous forces) [16, 17, 39] or (b) large values of the interfacial dilatational viscosity [14, 40]. Our derivation is focused on large Ma limit and it is similar to the derivation presented in [16, 17]. In addition to the incompressibility of the surfactant, we assume it to be insoluble, both inside and outside the drops and non-diffusing (the interfacial diffusivity of the surfactant is zero or the surface Péclet number is infinity). Since the interfacial tension is a function of the surfactant concentration, we can expand the former as follows

$$\delta\sigma = (\sigma - \sigma_0) = \left(\frac{d\sigma}{d\Gamma}\right)_{\Gamma=\Gamma_0} (\Gamma - \Gamma_0) = \left(\frac{d\sigma}{d\Gamma}\right)_{\Gamma=\Gamma_0} \delta\Gamma, \tag{A1}$$

where Γ_0 and $\sigma_0 = \sigma(\Gamma_0)$ are the reference surfactant concentration and the interfacial tension, respectively. The above equation can be rewritten as

$$\frac{\delta\Gamma}{\Gamma_0} = -Ma^{-1}\frac{\delta\sigma}{\tau a}, \tag{A2}$$

where the Marangoni number (Ma) is the ratio of the surfactant elasticity (E) and the capillary number (Ca)

$$Ma = \frac{E}{Ca};\ E = -\frac{\Gamma_0}{\sigma_0}\left(\frac{d\sigma}{d\Gamma}\right)_{\Gamma=\Gamma_0};\ Ca = \frac{\tau a}{\sigma_0}. \tag{A3}$$

Here, τ denotes the characteristic bulk viscous stresses while a is the characteristic length scale of the problem. From the tangential stress boundary condition, Eq. (6), we deduce that

$$\frac{\delta\sigma}{\tau a} \sim O\left(1\right). \tag{A4}$$

From this equation and Eq. (A2), we conclude that

$$\frac{\delta\Gamma}{\Gamma_0} \sim O\left(Ma^{-1}\right). \tag{A5}$$

In the limit of very large Ma, finite changes in the interfacial tension are caused by the infinitesimal changes in the surfactant concentration, and this is how the Marangoni stresses develop at the interface [16, 17]. Hence, it is reasonable to assume that the surfactant is uniformly distributed over the interface, i.e., $\Gamma = \Gamma_0$. Using this condition, the transport equation for an insoluble, non-diffusing and incompressible surfactant over the surface of a stationary and non-deforming drop reduces to Eq. (5). Since the typical value of the surfactant elasticity is $E \sim O\left(1\right)$, from Eq. (A3), we conclude that the small values of Capillary number ($Ca \ll 1$) correspond to the large values of Marangoni number ($Ma \gg 1$) or the incompressible surfactant limit. This limit for the small molecular weight surfactants results from their large Marangoni numbers since the dilatational viscosity of these surfactants is not large. But, this limit for the large molecular weight surfactants is due to their large dilatational viscosity.

Appendix B: Faxén's Laws for a drop covered with an incompressible surfactant

In this section, we derive the Faxén's laws for a drop covered with an incompressible surfactant. For this purpose, one can use the Lorentz reciprocal theorem for Stokes flows with a suitable choice of the auxiliary problem [15, 41–44]. However, in this work, we use the Lamb's general solution to derive Faxén's laws for a spherical surfactant-laden-drop. This approach is used earlier to derive the Faxén's laws for drops with a clean interface [45] and for drops covered with a surfactant, without any interfacial viscosity [46]. Accordingly, we

consider a drop covered with an incompressible surfactant, translating with velocity $\mathbf{U}$ in an arbitrary ambient flow field $\mathbf{V}_\infty$. In a frame of reference fixed at the center of the drop, the flow fields inside and outside of the drop should satisfy the Stokes equations along with an incompressibility condition

$$\mu_e \nabla^2 \mathbf{v}^{(e)} = \nabla p^{(e)}, \ \nabla \cdot \mathbf{v}^{(e)} = 0, \tag{B1}$$

$$\mu_i \nabla^2 \mathbf{v}^{(i)} = \nabla p^{(i)}, \ \nabla \cdot \mathbf{v}^{(i)} = 0. \tag{B2}$$

The flow field far away from the drop should approach the ambient flow field

$$\mathbf{v}^{(e)} = \mathbf{v}_\infty = \mathbf{V}_\infty - \mathbf{U}, \ \text{as} \ r \to \infty. \tag{B3}$$

These flow fields should satisfy the boundary conditions at the interface given by [45, 46]

$$\mathbf{v}^{(e)*} = \mathbf{v}^{(i)*}, \tag{B4a}$$

$$v_r^{(e)*} = v_r^{(i)*} = 0, \tag{B4b}$$

$$\nabla_S \cdot \mathbf{v}_S^* = 0, \tag{B4c}$$

$$\mathbf{T}_{(r)}^{(i)*} - \mathbf{T}_{(r)}^{(e)*} = \left[\nabla_S \sigma\right]^* + \mu_S \mathbf{w}_S^* + f\left(\sigma, \mathbf{v}\right) \mathbf{e}_r, \tag{B4d}$$

where $\mathbf{T}_{(r)}^{(k)} = \mathbf{e}_r \cdot \mathbf{T}^{(k)}$, $\mathbf{w}_S = \frac{2\mathbf{v}_S}{r^2} + \mathbf{e}_\theta \frac{1}{r\sin(\theta)} \frac{\partial \varpi}{\partial \phi} - \mathbf{e}_\phi \frac{1}{r} \frac{\partial \varpi}{\partial \theta}$ and $\varpi = \frac{1}{r\sin(\theta)} \left(\frac{\partial v_\theta}{\partial \phi} - \frac{\partial}{\partial \theta} \left(\sin\left(\theta\right) v_\phi \right) \right)$. Also, $(\,)^*$ denotes that the variables are evaluated at the interface and $f\left(\sigma, \mathbf{v}\right)$ denotes the terms which contribute to the normal stress balance at the interface. Since, we assume the drop to be spherical, our solution does not satisfy the normal stress boundary condition, instead this condition can be used to determine the leading order interface deformation. As the governing equations and boundary conditions are linear, we initially write the exterior flow field as $\mathbf{v}^{(e)} = \mathbf{v}_\infty + \mathbf{V}$ (similarly $p^{(e)} = p + p_\infty$). Assuming that the ambient flow field satisfies the Stokes equations, we see that the disturbance flow field also satisfies the Stokes equations. Using the Lamb's general solution, we write the disturbance flow field as

$$\mathbf{V} = \sum_{n=1}^{\infty} \left[\nabla \times \left(\mathbf{r} \chi_{-n-1} \right) + \nabla \Phi_{-n-1} - \frac{(n-2)}{2n\left(2n-1\right)\mu_e} r^2 \nabla p_{-n-1} + \frac{n+1}{n\left(2n-1\right)\mu_e} \mathbf{r} p_{-n-1} \right], \tag{B5a}$$

and

$$p = \sum_{n=0}^{\infty} p_n. \tag{B5b}$$

As the flow field interior to the drop also satisfies the Stokes equations, we have

$$\mathbf{v}^{(i)} = \sum_{n=0}^{\infty} \left[\nabla \times (\mathbf{r}\chi_n) + \nabla\Phi_n + \frac{n+3}{2\,(n+1)\,(2n+3)\,\mu_i} r^2 \nabla p_n - \frac{n}{(n+1)\,(2n+3)\,\mu_i} \mathbf{r} p_n \right], \tag{B6a}$$

and

$$p^{(i)} = \sum_{n=0}^{\infty} p_n. \tag{B6b}$$

Similarly, we can write the ambient flow field as

$$\mathbf{v}_\infty = \sum_{n=-\infty}^{n=\infty} \left[\nabla \times (\mathbf{r}\chi_n^\infty) + \nabla\Phi_n^\infty + \frac{n+3}{2\,(n+1)\,(2n+3)\,\mu_e} r^2 \nabla p_n^\infty - \frac{n}{(n+1)\,(2n+3)\,\mu_e} \mathbf{r} p_n^\infty \right], \tag{B7a}$$

and

$$p_\infty = \sum_{n=-\infty}^{n=\infty} p_n^\infty, \tag{B7b}$$

where $(\chi_{-n-1}, \Phi_{-n-1}, p_{-n-1})$ and $(\chi_n, \Phi_n, p_n, \chi_n^\infty, \Phi_n^\infty, p_n^\infty)$ are the solid spherical harmonics of degree $-n-1$ and n, respectively. We hereby rewrite the boundary conditions at the interface, Eq. (B4) as

$$\mathbf{v}^{(i)*} \cdot \mathbf{e}_r = 0, \tag{B8a}$$

$$\mathbf{V}^* \cdot \mathbf{e}_r + \mathbf{v}_\infty^* \cdot \mathbf{e}_r = 0, \tag{B8b}$$

$$\left[r \frac{\partial v_r^{(i)}}{\partial r} \right]^* = 0, \tag{B8c}$$

$$-\left[r \frac{\partial V_r}{\partial r} \right]^* = \left[r \frac{\partial v_{\infty r}}{\partial r} \right]^*, \tag{B8d}$$

$$\left[\mathbf{r} \cdot \nabla \times \mathbf{v}^{(i)} \right]^* - \left[\mathbf{r} \cdot \nabla \times \mathbf{V} \right]^* = \left[\mathbf{r} \cdot \nabla \times \mathbf{v}_\infty \right]^*, \tag{B8e}$$

$$\left[\mathbf{r} \cdot \nabla \times \mathbf{T}_{(r)}^{(i)} \right]^* - \left[\mathbf{r} \cdot \nabla \times \boldsymbol{\pi}_{(r)} \right]^* = \mu_S \left[\mathbf{r} \cdot \nabla \times \mathbf{w}_S \right]^* + \left[\mathbf{r} \cdot \nabla \times \boldsymbol{\pi}_{\infty(r)} \right]^*, \tag{B8f}$$

$$\begin{aligned} &\left[\mathbf{r} \cdot \nabla \times \left(\mathbf{r} \times \mathbf{T}_{(r)}^{(i)} \right) \right]^* - \left[\mathbf{r} \cdot \nabla \times \left(\mathbf{r} \times \boldsymbol{\pi}_{(r)} \right) \right]^* \\ &= \left[\mathbf{r} \cdot \nabla \times (\mathbf{r} \times \nabla_S \sigma) \right]^* + \mu_S \left[\mathbf{r} \cdot \nabla \times (\mathbf{r} \times \mathbf{w}_S) \right]^* + \left[\mathbf{r} \cdot \nabla \times \left(\mathbf{r} \times \boldsymbol{\pi}_{\infty(r)} \right) \right]^*. \end{aligned} \tag{B8g}$$

Substituting Eqs. (B5)-(B7) into Eqs. (B8), we obtain a set of seven equations. From Eq. (B8a), we obtain

$$\sum_{n=1}^{\infty} \left\{ \frac{na}{2\,(2n+3)\,\mu_i} p_n^* + \frac{n}{a} \Phi_n^* \right\} = 0. \tag{B9a}$$

From Eq. (B8b), we obtain

$$\sum_{n=1}^{\infty}\left\{\frac{(n+1)\,a}{2\,(2n-1)\,\mu_e}p_{-n-1}^{*}-\frac{(n+1)}{a}\Phi_{-n-1}^{*}\right\}=-\sum_{n=\infty}^{\infty}\left\{\frac{na}{2\,(2n+3)\,\mu_e}p_n^{\infty *}+\frac{n}{a}\Phi_n^{\infty *}\right\}. \quad \text{(B9b)}$$

From Eq. (B8c), we obtain

$$\sum_{n=1}^{\infty}\left[\frac{n\,(n+1)\,a}{2\,(2n+3)\,\mu_i}p_n^{*}+\frac{n\,(n-1)}{a}\Phi_n^{*}\right]=0. \quad \text{(B9c)}$$

From Eq. (B8d), we obtain

$$\sum_{n=1}^{\infty}\left[\frac{n\,(n+1)\,a}{2\,(2n-1)\,\mu_e}p_{-n-1}^{*}-\frac{(n+1)\,(n+2)}{a}\Phi_{-n-1}^{*}\right]=\sum_{n=-\infty}^{\infty}\left[\frac{n\,(n+1)\,a}{2\,(2n+3)\,\mu_e}p_n^{\infty *}+\frac{n\,(n-1)}{a}\Phi_n^{\infty *}\right]. \quad \text{(B9d)}$$

From Eq. (B8e), we obtain

$$\sum_{n=1}^{\infty}\left\{n\,(n+1)\left[\chi_n^{*}-\chi_{-n-1}^{*}\right]\right\}=\sum_{n=-\infty}^{n=\infty}n\,(n+1)\,\chi_n^{\infty *}. \quad \text{(B9e)}$$

From Eq. (B8f), we obtain

$$\begin{aligned}&\sum_{n=1}^{\infty}\left\{n\,(n+1)\left[\lambda\,(n-1)\,\chi_n^{*}+(n+2)\,\chi_{-n-1}^{*}\right]\right\}+\sum_{n=1}^{\infty}\beta n\,(n+2)\,(n^2-1)\,\chi_n^{*}\\&=\sum_{n=-\infty}^{\infty}(n-1)\,n\,(n+1)\,\chi_n^{\infty *}.\end{aligned} \quad \text{(B9f)}$$

From Eq. (B8g), we obtain

$$\begin{aligned}&\sum_{n=1}^{\infty}\left\{\frac{2n\,(n+1)\,(n+2)}{a}\Phi_{-n-1}^{*}-\frac{(n+1)^2\,(n-1)\,a}{(2n-1)\,\mu_e}p_{-n-1}^{*}\right\}\\&+\sum_{n=1}^{\infty}\left\{\frac{2\lambda}{a}\,(n-1)\,n\,(n+1)\,\Phi_n^{*}+\frac{n^2\,(n+2)\,a\lambda}{(2n+3)\,\mu_i}p_n^{*}\right\}\\&+\sum_{n=1}^{\infty}\left\{-\beta\frac{(n+3)\,na}{(2n+3)\,\mu_i}p_n^{*}-\frac{2n\,(n+1)\,\beta}{a}\Phi_n^{*}\right\}+\frac{\left[\mathbf{r}\cdot\nabla\times(\mathbf{r}\times\nabla_S\sigma)\right]^{*}}{\mu_e}\\&=\sum_{n=-\infty}^{n=\infty}\left\{\frac{2}{a}\,(n-1)\,n\,(n+1)\,\Phi_n^{\infty *}+\frac{n^2\,(n+2)\,a}{(2n+3)\,\mu_e}p_n^{\infty *}\right\}.\end{aligned} \quad \text{(B9g)}$$

The solid spherical harmonics are defined as [45, 46]

$$p_n=A_n\mu_i a^{-n-1}r^n S_n\left(\theta,\phi\right), \quad \text{(B10a)}$$

$$p_{-n-1}=A_{-n-1}\mu_e a^n r^{-n-1}S_n\left(\theta,\phi\right), \quad \text{(B10b)}$$

$$\Phi_n = B_n a^{-n+1} r^n S_n(\theta,\phi), \tag{B10c}$$

$$\Phi_{-n-1} = B_{-n-1} a^{n+2} r^{-n-1} S_n(\theta,\phi), \tag{B10d}$$

$$\chi_n = C_n a^{-n} r^n S_n(\theta,\phi), \tag{B10e}$$

$$\chi_{-n-1} = C_{-n-1} a^{n+1} r^{-n-1} S_n(\theta,\phi), \tag{B10f}$$

$$p_n^\infty = \frac{2(2n+3)}{n} \alpha_n \mu_e a^{-n-1} r^n S_n(\theta,\phi), \tag{B10g}$$

$$\Phi_n^\infty = \frac{1}{n} \beta_n a^{-n+1} r^n S_n(\theta,\phi), \tag{B10h}$$

$$\chi_n^\infty = \frac{1}{n(n+1)} \gamma_n a^{-n} r^n S_n(\theta,\phi). \tag{B10i}$$

Furthermore, we expand the interfacial tension in terms of surface spherical harmonics as

$$\sigma = \sum_{n=0}^{\infty} \sigma_n S_n(\theta,\phi). \tag{B11}$$

Note that, we used a shorthand notation for terms of the form $A_n S_n(\theta,\phi)$ to represent a sum of $2n+1$ terms as given below

$$A_n S_n(\theta,\phi) = \sum_{m=0}^{n} \left(A_n^m \cos(m\phi) + \hat{A}_n^m \sin(m\phi) \right) P_n^m(\cos(\theta)), \tag{B12}$$

where $P_n^m(\cos(\theta))$ is the associated Legendre polynomial of order m and degree n. We substitute Eqs. (B10) and (B11) into Eq. (B9) and solve for the unknown constants A_n^m, B_n^m, C_n^m, A_{-n-1}^m, B_{-n-1}^m, C_{-n-1}^m and σ_n^m (and the corresponding variables with carat over them) in terms of the constants α_n^m, β_n^m and γ_n^m. The result of this procedure is the following equations

$$A_n^m = 0, \tag{B13a}$$

$$B_n^m = 0, \tag{B13b}$$

$$C_n^m = \frac{2n\gamma_n^m + \gamma_n^m}{n(n+1)\left[\beta n^2 + (\beta+\lambda+1)n - 2\beta - \lambda + 2\right]}, \tag{B13c}$$

$$A_{-n-1}^m = -\frac{2(2n-1)\left[n(\alpha_n^m + \beta_n^m) + \frac{1}{2}\beta_n^m + \frac{3}{2}\alpha_n^m + \alpha_{-n-1}^m\right]}{n+1}, \tag{B13d}$$

$$B_{-n-1}^m = \frac{(-2\beta_n^m - 2\alpha_n^m)n + \beta_n^m - \alpha_n^m + 2\beta_{-n-1}^m}{2n+2}, \tag{B13e}$$

$$C_{-n-1}^m = \frac{\left\{ \begin{array}{l} -\beta\left(\gamma_{-n-1}^m + \gamma_n^m\right) n^2 + \left[\left(-\gamma_{-n-1}^m - \gamma_n^m\right)\beta + (-\lambda-1)\gamma_{-n-1}^m - \gamma_n^m(\lambda-1)\right] n \\ + \left(2\gamma_n^m + 2\gamma_{-n-1}^m\right)\beta + (\lambda-2)\gamma_{-n-1}^m + (\lambda-1)\gamma_n^m \end{array} \right\}}{n(n+1)\left[\beta n^2 + (\beta+\lambda+1)n - 2\beta - \lambda + 2\right]}, \tag{B13f}$$

$$\sigma_n^m = -\frac{2\,(2n+1)\left[(\alpha_n^m+\beta_n^m)\,n-\frac{1}{2}\beta_n^m+\frac{3}{2}\alpha_n^m\right]\mu_e}{n\,(n+1)}. \tag{B13g}$$

From Eq. (B13), we can make few deductions. Noting that $\gamma_{-2}^m = 0$, we find that $C_{-2}^m = -\frac{1}{2}\gamma_{-2}^m = 0$. As the torque experienced by the drop is given by $\mathbf{T} = -8\pi\mu_e\nabla\,(r^3\chi_{-2}) = 0$, we find that the drop covered with an incompressible surfactant does not experience any hydrodynamic torque. Furthermore, we note the following equation holds

$$A_{-n-1}^m\big|_{\substack{\text{drop covered with an}\\ \text{incompressible surfactant}}} = A_{-n-1}^m\big|_{\text{rigid sphere}} \tag{B14}$$

Using the equations for force and stresslet experienced by a drop, $\mathbf{F} = -4\pi\nabla\,(r^3 p_{-2})$, $\mathbf{S} = -\frac{2\pi}{3}\nabla\nabla\,(r^5 p_{-3})$ and Eq. (B10b), we conclude that the force and stresslet experienced by a translating drop covered with an incompressible surfactant are the same as those experienced by a translating rigid sphere. In summary, we hereby provide the Faxén's laws for a drop of radius a covered with an insoluble, non-diffusing and incompressible surfactant as

$$\mathbf{F} = 6\pi\mu_e a\left(1+\frac{a^2\nabla^2}{6}\right)\mathbf{V}_\infty|_O - 6\pi\mu_e a\mathbf{U}, \tag{B15a}$$

$$\mathbf{T} = \mathbf{0}, \tag{B15b}$$

$$\mathbf{S} = \frac{20}{3}\pi\mu_e a^3\left(1+\frac{a^2\nabla^2}{10}\right)\mathbf{E}_\infty|_O, \tag{B15c}$$

where the subscript O denotes that the quantities are evaluated at the center of the drop and $\mathbf{E}_\infty$ denotes the rate of strain field of the ambient flow field.

For zero surface viscosity, we would like to compare this flow field due to an isolated translating drop covered with an incompressible, insoluble, and non-diffusing surfactant in an arbitrary ambient flow field with that reported in the literature [17]. For this purpose, we note that

$$\begin{aligned}
\left\{A_n^m, B_n^m, A_{-n-1}^m, B_{-n-1}^m\right\}\big|_{\substack{\text{drop covered with an}\\ \text{incompressible surfactant}}} &= \left\{A_n^m, B_n^m, A_{-n-1}^m, B_{-n-1}^m\right\}\big|_{\text{rigid sphere}},\\
\left\{C_n^m, C_{-n-1}^m\right\}\big|_{\substack{\text{drop covered with an incompressible}\\ \text{surfactant and } \beta=0}} &= \left\{C_n^m, C_{-n-1}^m\right\}\big|_{\text{clean drop}}.
\end{aligned} \tag{B16}$$

Also, note that the flow field using Lamb's general solution, Eqs. (B5a), (B6a), and (B7a) can be written as a sum of the surface solenoidal and the surface irrotational flow fields on the family of concentric spherical surfaces

$$\mathbf{v} = \mathbf{v}^{Sol} + \mathbf{v}^{Irr}, \tag{B17}$$

where

$$\mathbf{v}^{Sol} = \sum_{n=-\infty}^{\infty} \nabla \times (\mathbf{r}\,\chi_n),$$
$$\mathbf{v}^{Irr} = \sum_{n=-\infty}^{\infty} \left[\nabla\Phi_n + \frac{n+3}{2\,(n+1)\,(2n+3)\,\mu} r^2 \nabla p_n - \frac{n}{(n+1)\,(2n+3)\,\mu}\mathbf{r}\,p_n\right].$$

Here $\mathbf{v}^{Sol}$ and $\mathbf{v}^{Irr}$ satisfy the conditions

$$\begin{aligned} &\mathbf{i}_r \cdot \left(\nabla_S \times \mathbf{v}^{Irr}\right) = 0, \\ &\nabla_S \cdot \mathbf{v}^{Sol} = 0;\ \mathbf{i}_r \cdot \mathbf{v}^{Sol} = 0. \end{aligned} \tag{B18}$$

In lieu of Eqs. (B10), (B16), and (B17), we conclude that the surface solenoidal flow field due to a surfactant-laden-drop with zero surface viscosity is the same as that due to a clean drop. Similarly, the surface irrotational flow field due to a surfactant-laden-drop is the same as that due to a rigid sphere. These results agree with the general solution due to a drop covered with incompressible, insoluble and non-diffusing surfactant with zero surface viscosity, as derived by Blawzdziewicz *et al* [17].

One can understand the peculiar behavior of the translating surfactant-laden-drops, in an arbitrary ambient flow, experiencing the same force and stresslet as that of rigid spheres in a similar configuration as follows. As shown earlier, any flow past a particle, irrespective of the boundary conditions on the particle (i.e., the particle can be a rigid particle, a drop or a surfactant-laden-drop), can be decomposed into a surface solenoidal flow field and a surface irrotational flow field on the family of concentric spherical surfaces. The surface irrotational flow field is torque-free and it exerts a force and a stresslet on the particle whereas the surface solenoidal flow field is force-free and stresslet-free and it exerts a torque on the particle. For a drop (both clean and surfactant laden), the surface solenoidal flow field is torque-free too. For a drop covered with an incompressible surfactant with zero surfactant diffusivity, the surface irrotational flow field due to a surfactant-laden-drop is the same as that due to a rigid sphere. Due to this reason, the force and the stresslet experienced by a surfactant-laden-drop are independent of the viscosity ratio and the interfacial viscosity; also this force and stresslet are the same as those experienced by a rigid sphere.

ACKNOWLEDGMENTS

We would like to thank Dr. Sangtae Kim, Dr. Uddipta Ghosh and Mr. Shubhadeep Mandal for useful discussions. We would also like to thank Mr. Nikhil Desai for his help in editing this manuscript. This research is supported by grants from The Gulf of Mexico Research Initiative and the National Science Foundation, CBET-1445955-CAREER and CBET-1604423.

---

[1] L. Gary Leal, *Advanced Transport Phenomena. Fluid Mechanics and Convective Transport Processes* (Cambridge University Press, 2010).

[2] Sangtae Kim and Seppo Karrila, *Microhydrodynamics: Principles and Selected Applications* (Butterworth-Heinemann, 1991).

[3] Eric Lauga and Thomas R. Powers, "The hydrodynamics of swimming microorganisms," Reports on Progress in Physics **72**, 096601 (2009).

[4] Allen T. Chwang and T. Yao-Tsu Wu, "Hydromechanics of low-Reynolds-number flow. Part 2. Singularity method for Stokes flows," Journal of Fluid Mechanics **67**, 787–815 (1975).

[5] S. H. Lee, R. S. Chadwick, and L. Gary Leal, "Motion of a sphere in the presence of a plane interface. Part 1. An approximate solution by generalization of the method of Lorentz," Journal of Fluid Mechanics **93**, 705–726 (1979).

[6] S.-M. Yang and L.G. Leal, "Motions of a fluid drop near a deformable interface," International Journal of Multiphase Flow **16**, 597–616 (1990).

[7] Allison P. Berke, Linda Turner, Howard C. Berg, and Eric Lauga, "Hydrodynamic Attraction of Swimming Microorganisms by Surfaces," Physical Review Letters **101**, 038102 (2008).

[8] Diego Lopez and Eric Lauga, "Dynamics of swimming bacteria at complex interfaces," Physics of Fluids **26**, 071902 (2014).

[9] Saverio E. Spagnolie and Eric Lauga, "Hydrodynamics of self-propulsion near a boundary: predictions and accuracy of far-field approximations," Journal of Fluid Mechanics **700**, 105–147 (2012).

[10] Ian M. Head, D. Martin Jones, and Wilfred F. M. Röling, "Marine microorganisms make a meal of oil," Nature Reviews Microbiology **4**, 173–182 (2006).

[11] T.S. Awad, H.A. Moharram, O.E. Shaltout, D. Asker, and M.M. Youssef, "Applications of ultrasound in analysis, processing and quality control of food: A review," Food Research International **48**, 410–427 (2012).

[12] R. Shankar Subramanian and R. Balasubramaniam, *The Motion of Bubbles and Drops in Reduced Gravity* (Cambridge University Press, 2005).

[13] James A. Hanna and Petia M. Vlahovska, "Surfactant-induced migration of a spherical drop in Stokes flow," Physics of Fluids **22**, 013102 (2010).

[14] Jonathan T. Schwalbe, Frederick R. Phelan, Jr., Petia M. Vlahovska, and Steven D. Hudson, "Interfacial effects on droplet dynamics in Poiseuille flow," Soft Matter **7**, 7797–7804 (2011).

[15] On Shun Pak, Jie Feng, and Howard A. Stone, "Viscous Marangoni migration of a drop in a Poiseuille flow at low surface Péclet numbers," Journal of Fluid Mechanics **753**, 535–552 (2014).

[16] Jerzy Bławzdziewicz, Vittorio Cristini, and Michael Loewenberg, "Stokes flow in the presence of a planar interface covered with incompressible surfactant," Physics of Fluids **11**, 251–258 (1999).

[17] J. Blawzdziewicz, E. Wajnryb, and Michael Loewenberg, "Hydrodynamic interactions and collision efficiencies of spherical drops covered with an incompressible surfactant film," Journal of Fluid Mechanics **395**, 29–59 (1999).

[18] José A. Ramirez, Robert H. Davis, and Alexander Z. Zinchenko, "Microflotation of fine particles in the presence of a bulk-insoluble surfactant," International Journal of Multiphase Flow **26**, 891–920 (2000).

[19] Michael A. Rother and Robert H. Davis, "Buoyancy-driven coalescence of spherical drops covered with incompressible surfactant at arbitrary Péclet number," Journal of Colloid and Interface Science **270**, 205–220 (2004).

[20] J. Bławzdziewicz, P. Vlahovska, and M. Loewenberg, "Rheology of a dilute emulsion of surfactant-covered spherical drops," Physica A: Statistical Mechanics and its Applications **276**, 50–85 (2000).

[21] P. Vlahovska, J. Blawzdziewicz, and M. Loewenberg, "Nonlinear rheology of a dilute emulsion of surfactant-covered spherical drops in time-dependent flows," Journal of Fluid Mechanics **463**, 1–24 (2002).

[22] Vittorio Cristini, J. Blawzdziewicz, and Michael Loewenberg, "Near-contact motion of surfactant-covered spherical drops," Journal of Fluid Mechanics **366**, 259–287 (1998).

[23] Alexander Z. Zinchenko, Michael A. Rother, and Robert H. Davis, "Gravity-induced collisions of spherical drops covered with compressible surfactant," Journal of Fluid Mechanics **667**, 369–402 (2011).

[24] M. Schmitt and H. Stark, "Marangoni flow at droplet interfaces: Three-dimensional solution and applications," Physics of Fluids **28**, 012106 (2016).

[25] John W. M. Bush and David L. Hu, "Walking on water: Biolocomotion at the Interface," Annual Review of Fluid Mechanics **38**, 339–369 (2006).

[26] Eric Lauga and Anthony M. J. Davis, "Viscous Marangoni propulsion," Journal of Fluid Mechanics **705**, 120–133 (2012).

[27] Hassan Masoud and Howard A. Stone, "A reciprocal theorem for Marangoni propulsion," Journal of Fluid Mechanics **741**, R4 (2014).

[28] J. R. Blake, "A note on the image system for a stokeslet in a no-slip boundary," Mathematical Proceedings of the Cambridge Philosophical Society **70**, 303–310 (1971).

[29] J. R. Blake and A. T. Chwang, "Fundamental singularities of viscous flow," Journal of Engineering Mathematics **8**, 23–29 (1974).

[30] K. Aderogba and J. R. Blake, "Action of a force near the planar surface between two semi-infinite immiscible liquids at very low Reynolds numbers," Bulletin of the Australian Mathematical Society **18**, 345–356 (1978).

[31] Yuris O. Fuentes, Sangtae Kim, and David J. Jeffrey, "Mobility functions for two unequal viscous drops in Stokes flow. I. Axisymmetric motions," Physics of Fluids **31**, 2445–2455 (1988).

[32] Yuris O. Fuentes, Sangtae Kim, and David J. Jeffrey, "Mobility functions for two unequal viscous drops in Stokes flow. II. Asymmetric motions," Physics of Fluids A: Fluid Dynamics **1**, 61–76 (1989).

[33] L.E. Scriven, "Dynamics of a fluid interface Equation of motion for Newtonian surface fluids," Chemical Engineering Science **12**, 98–108 (1960).

[34] David A. Edwards, Howard Brenner, and D. T. Wasan, *Interfacial Transport Processes and Rheology* (Bufferworth-Heinemann, 1991).

[35] Horace Lamb, *Hydrodynamics* (Cambridge University Press, 1932).

[36] Abdallah Daddi-Moussa-Ider and Stephan Gekle, "Hydrodynamic mobility of a solid particle near a spherical elastic membrane: Axisymmetric motion," Physical Review E **95**, 013108 (2017).

[37] H. A. Stone, "A simple derivation of the timedependent convectived-iffusion equation for surfactant transport along a deforming interface," Physics of Fluids A: Fluid Dynamics **2**, 111–112 (1990).

[38] Saverio E. Spagnolie, Gregorio R. Moreno-Flores, Denis Bartolo, and Eric Lauga, "Geometric capture and escape of a microswimmer colliding with an obstacle," Soft Matter **11**, 3396–3411 (2015).

[39] Harris Wong, David Rumschitzki, and Charles Maldarelli, "Marangoni effects on the motion of an expanding or contracting bubble pinned at a submerged tube tip," Journal of Fluid Mechanics **379**, 279–302 (1999).

[40] Shubhadeep Mandal and Suman Chakraborty, "Influence of interfacial viscosity on the dielectrophoresis of drops," Physics of Fluids **29**, 052002 (2017).

[41] H. Brenner, "The Stokes resistance of an arbitrary particleIV Arbitrary fields of flow," Chemical Engineering Science **19**, 703–727 (1964).

[42] J. M. Rallison, "Note on the Faxén relations for a particle in Stokes flow," Journal of Fluid Mechanics **88**, 529–533 (1978).

[43] S. Kim and S.-Y. Lu, "The functional similarity between faxén relations and singularity solutions for fluid-fluid, fluid-solid and solid-solid dispersions," International Journal of Multiphase Flow **13**, 837–844 (1987).

[44] Ali Nadim, Hossein Haj-Hariri, and Ali Borhan, "Thermocapillary migration of slightly deformed droplets," Particulate Science and Technology **8**, 191–198 (1990).

[45] G. Hetsroni and S. Haber, "The flow in and around a droplet or bubble submerged in an unbound arbitrary velocity field," Rheologica Acta **9**, 488–496 (1970).

[46] S. Haber and G. Hetsroni, "Hydrodynamics of a drop submerged in an unbounded arbitrary velocity field in the presence of surfactants," Applied Scientific Research **25**, 215–233 (1972).